High Power Lasers & Interactions

by

Professor Chris R. Chatwin

University of Sussex

School of Science & Technology - Keynote

SIXTH INTERNATIONAL CONFERENCE

ON

LASER SCIENCE & APPLICATIONS - ICLSA07

January 15-18, 2007

Cairo - Egypt

Summary

- Brief History & Evolution of Laser
- High Power Thermal Lasers
- Modelling Laser/Material Interactions
- High Power Thermal Lasers
- High Power Micro Machining

Brief History and Evolution of Lasers

- 1917 - Albert Einstein developed the concept of stimulated emission, which is the phenomenon used in lasers
- In 1954 the maser was the first device to use stimulated emission (Townes & Schawlow). Microwave amplification by stimulated emission of radiation

Brief History of Lasers

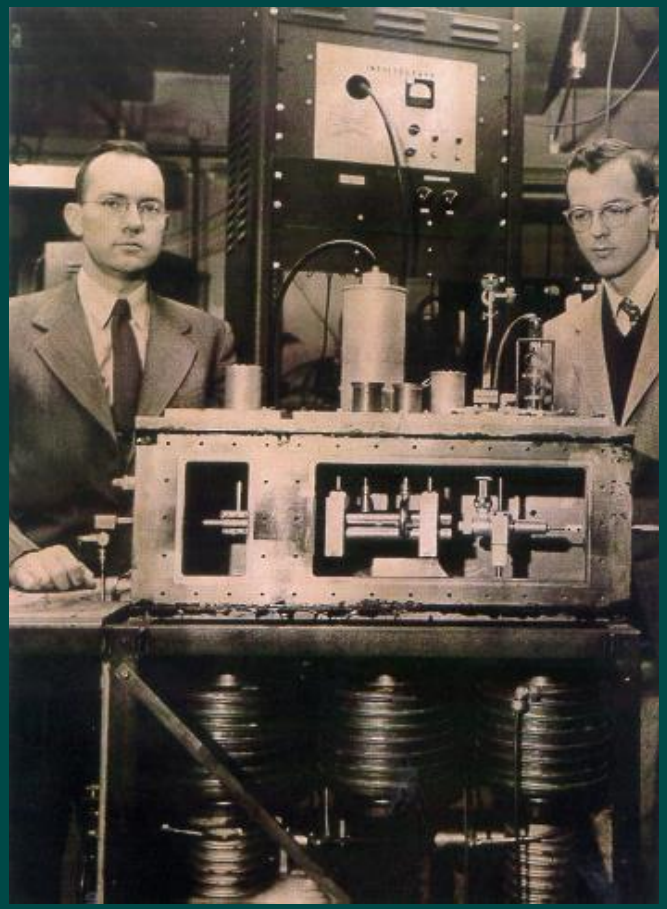

Charles Townes & Jim Gordon at Columbia University in 1954 with their second working MASER

- In 1958 Townes & Schawlow suggested that stimulated emission could be used in the infrared and optical portions of the spectrum
- The device was originally termed the optical maser
- This term was dropped in favour of LASER. Standing for Light Amplification by Stimulated Emission of Radiation

1st Laser - Ted Maiman 15th May 1960 - working alone and against the wishes of his boss at Hughes Research Laboratories

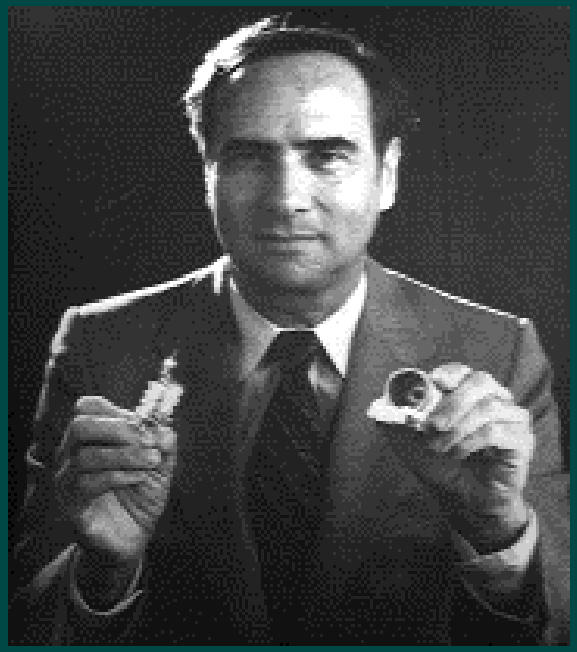

Electrical Engineer

Original Laboratory Set-Up for the Ruby Laser

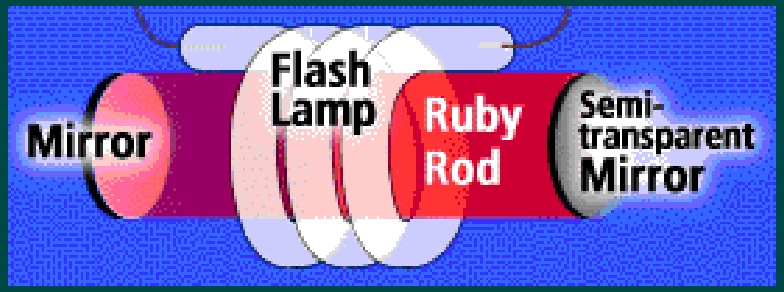

Maiman's Ruby Laser - 694.3 nm

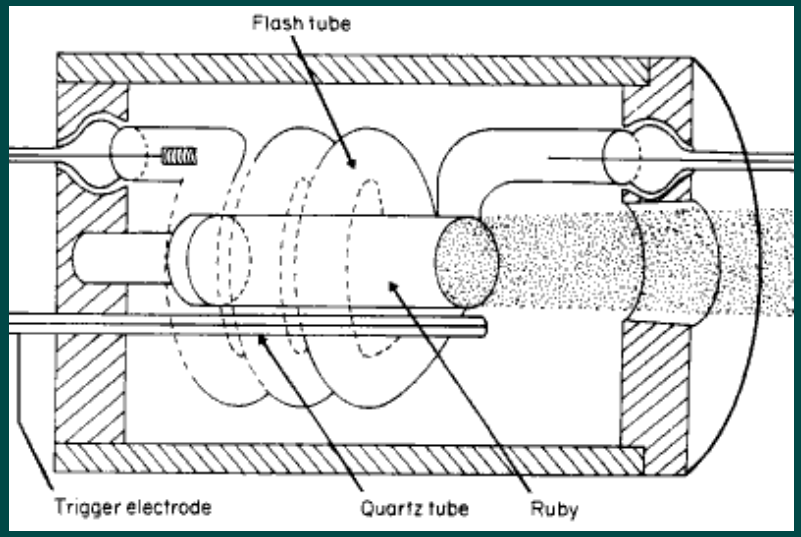

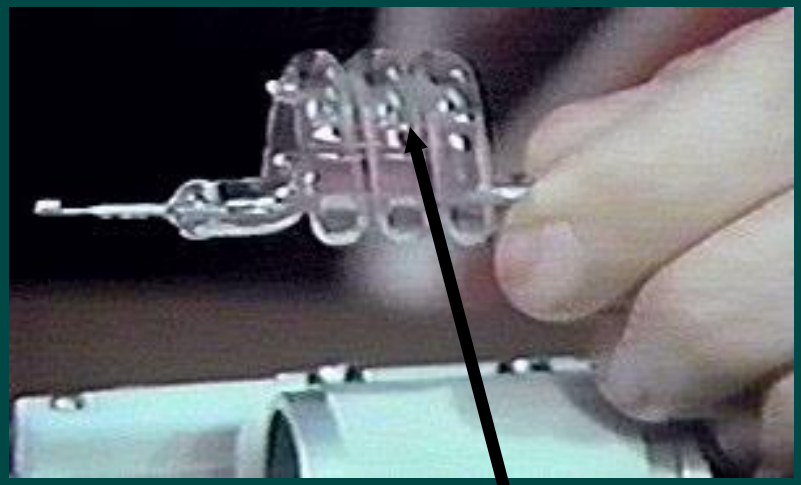

Synthetic pale pink ruby crystal Al_2O_3 containing about 0.05% by weight of Cr_2O_3

New York Times 8th July 1960, Wrong Ruby Crystal is shown here. The journalist didn't like the actual stubby crystal. This crystal was used later

Bell Labs & the Laser

1960 Ali Javan, William Bennet, Donald Herriot - HeNe Laser - 1st CW Laser - 1.15 μm

1961 Boyle & Nelson - Continuously operating Ruby Laser

1962 Kumar Patel (front), Faust, McFarlane, Bennet (left to right) - 5 Noble gas lasers and lasers using oxygen mixtures

Bell Labs & the Laser

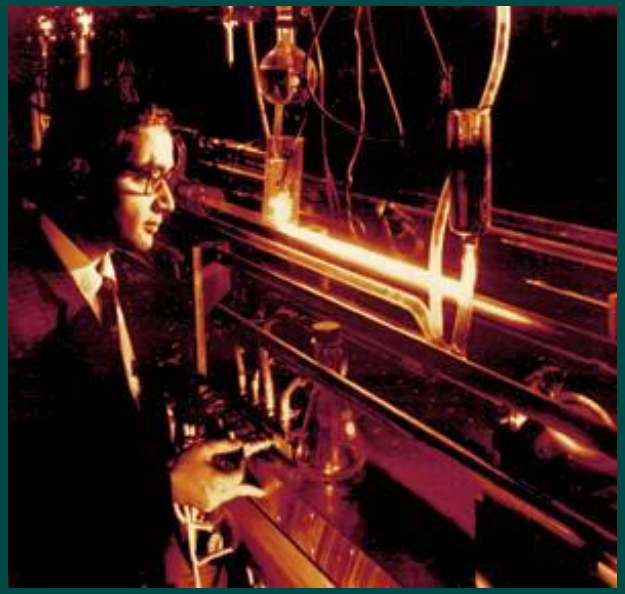

1964 C. K. N. Patel - High Power Carbon Dioxide Laser - 10.6μm

1971 Izuo Hayashsi & Morton Panish - first semiconductor laser that operated continuously at room temperature

1964: First Nd:YAG laser 1.06μm (uses neodymium doped yttrium aluminium garnet crystals) by J. F. Geusic and R. G. Smith

A Beam Focusing Lens and an Assist Gas Nozzle is required for all but the Excimer Laser

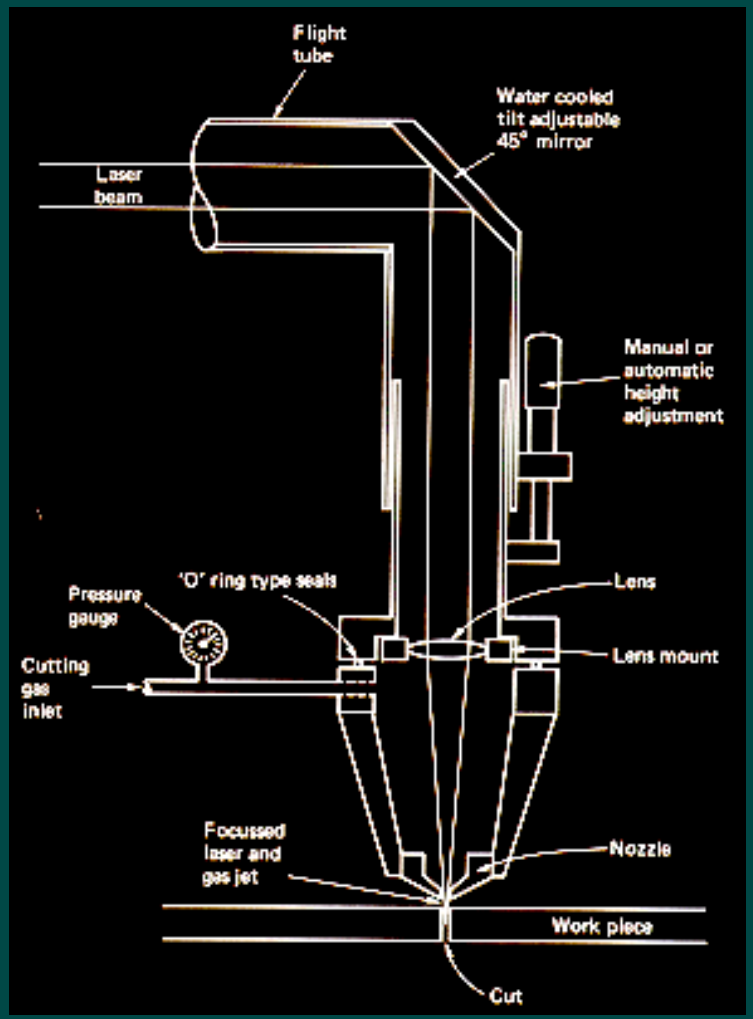

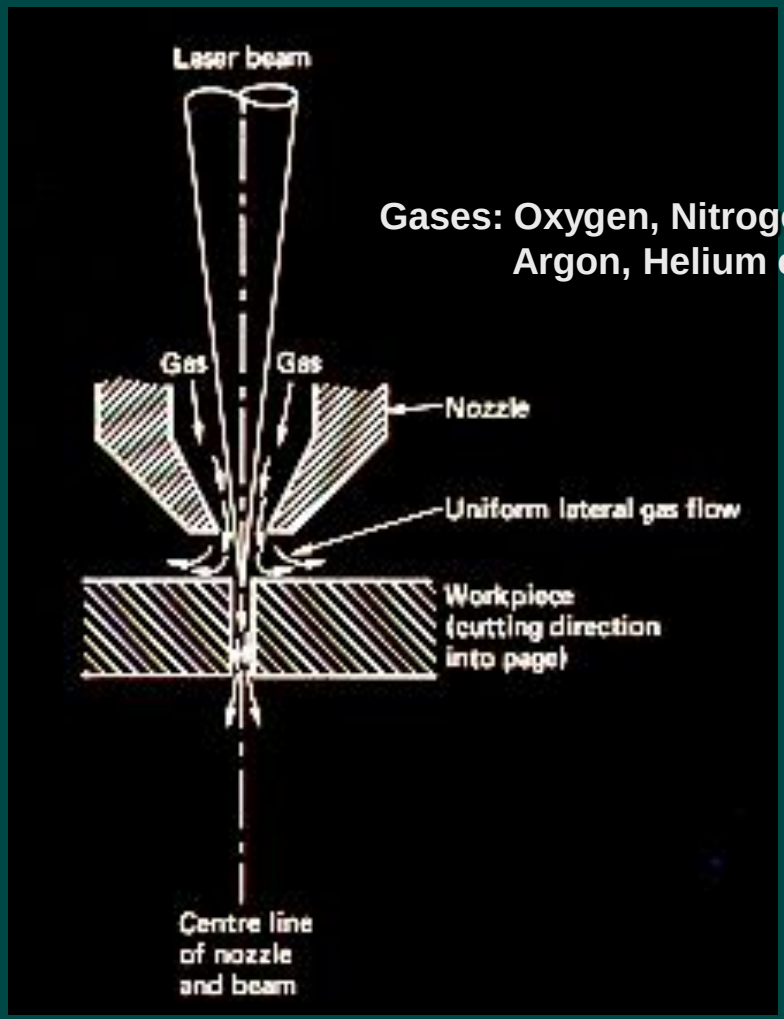

Gases: Oxygen, Nitrogen, Argon, Helium etc.

Dry Laser Etching Ablates Material by Bond Breaking

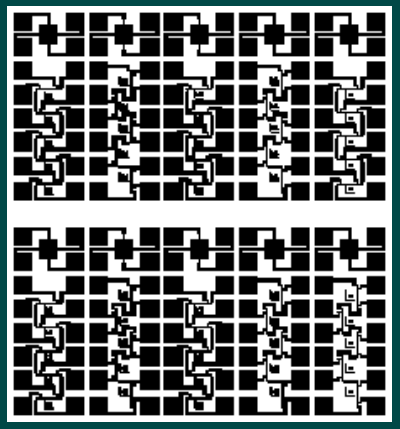

Chrome on Quartz Mask

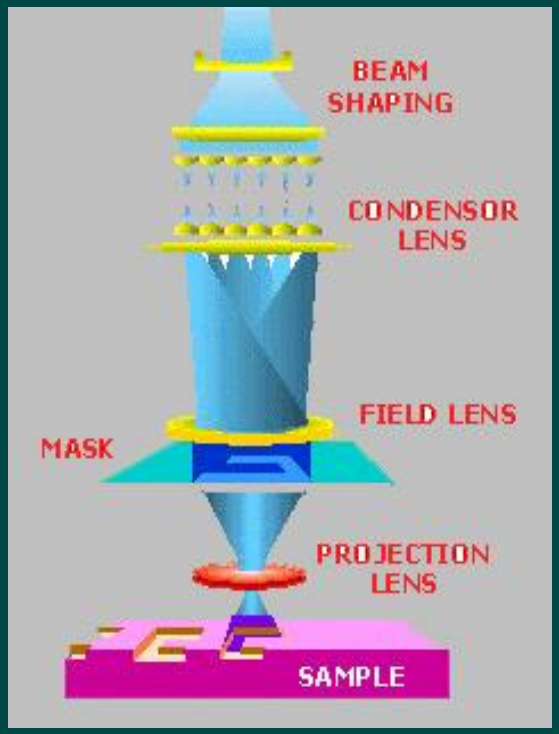

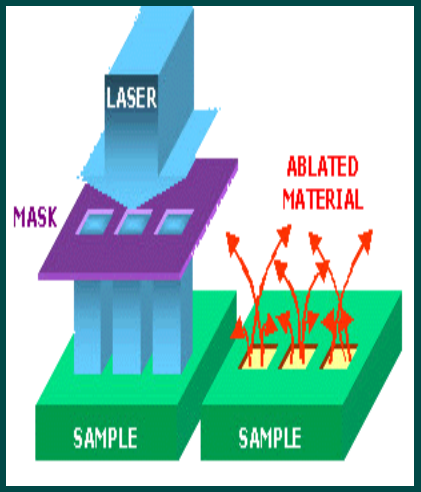

Lambda Physik LPX 201i, 125W mean power, 2.5J/pulse,100 Hz prf, 10 to 50 ns pulse width

Evolution of Industrial Lasers

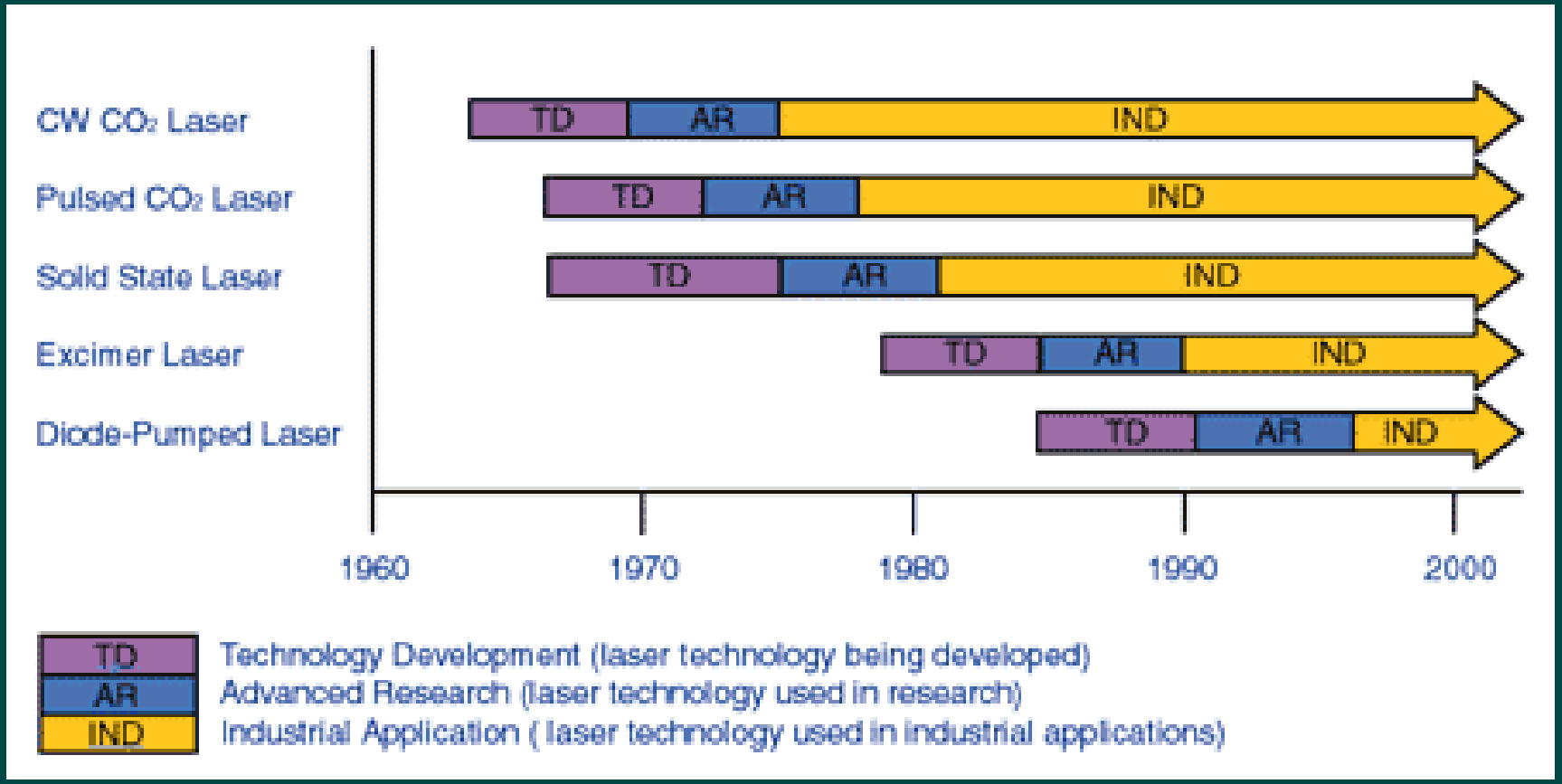

High Power Materials Processing Lasers

- Carbon Dioxide - up to 100kW more usually 2 to 7kW - 10.6μm
- Carbon Monoxide - not generally available, up to 5kW - 5 to 6μm
- Nd-YAG - up to 4.5kW - 1.06μm
- UV - Argon Ion 2W, HeCd, Tripled YAG 5W
- Diode Lasers 2 kW

High Power Micro-machining Lasers

- Copper Vapour Lasers 511& 578 nm, 20-30 ns pulses, 2-20kHz, 50 to 500 kW peak power
- Excimer - pulsed mean power 1kW – UV – 157nm, 193nm, 248nm,308nm, 351nm, 1000Hz, 1kW
- Nd-YVO_4 – 355nm Neodymium Vanadate 38ns pulses, 10kHz, 6 W mean
- Ti:Sapphire – 850nm , 250kHz, 100 fs pulses, 300kW,

Our Contribution to the Evolution of CO_2 Lasers

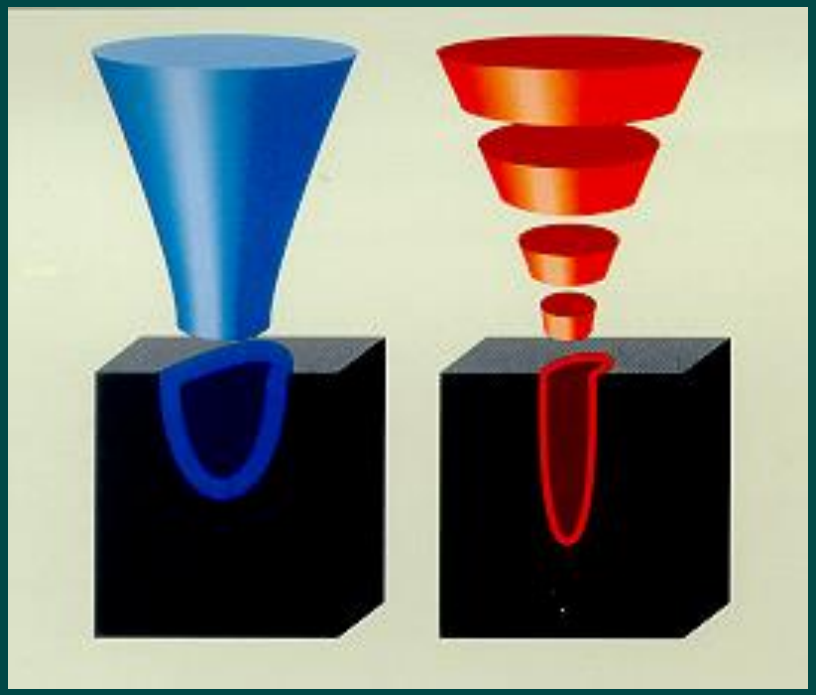

- Pulsed lasers give a sharper, hotter knife
- Narrower focus
- It gives greater process control
- High instantaneous power allows processing of highly reflective metals like aluminium

Prototype High Pulse Repetition Frequency (PRF), High Power CO_2 Laser

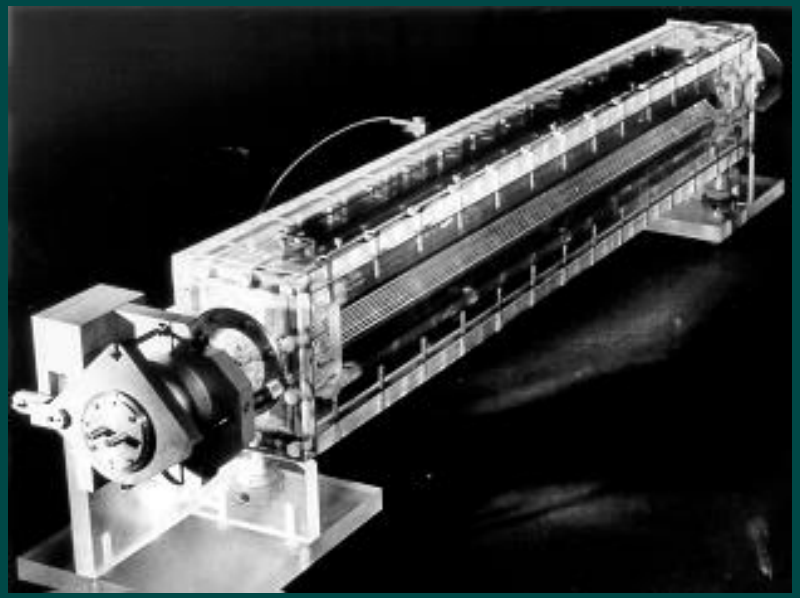

Prototype system that could run for a few seconds

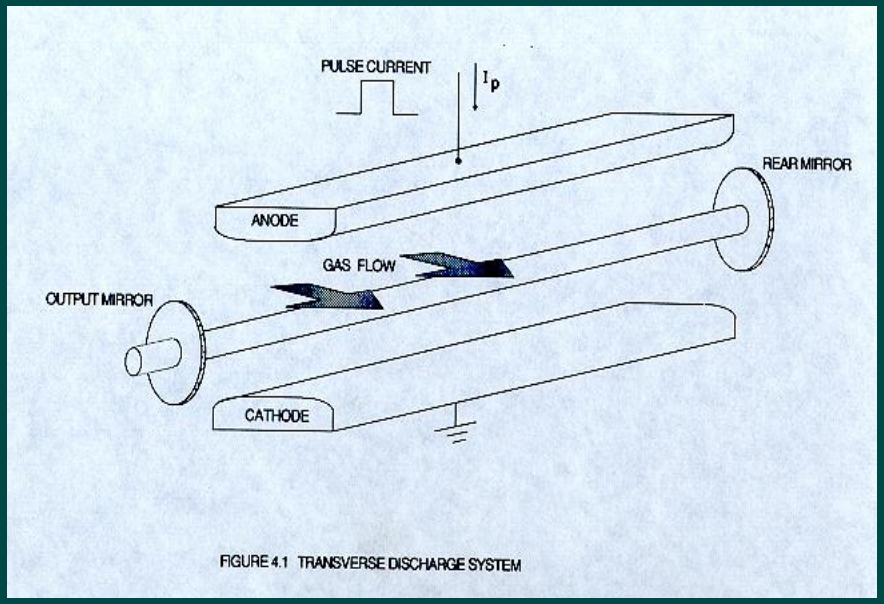

FIGURE 4.1 TRANSVERSE DISCHARGE SYSTEM

In order to run continuously the first prototype required a transverse gas flow

Computer Simulation was extremely important in establishing the Laser design specification

Energy level diagram of a Carbon Dioxide Laser

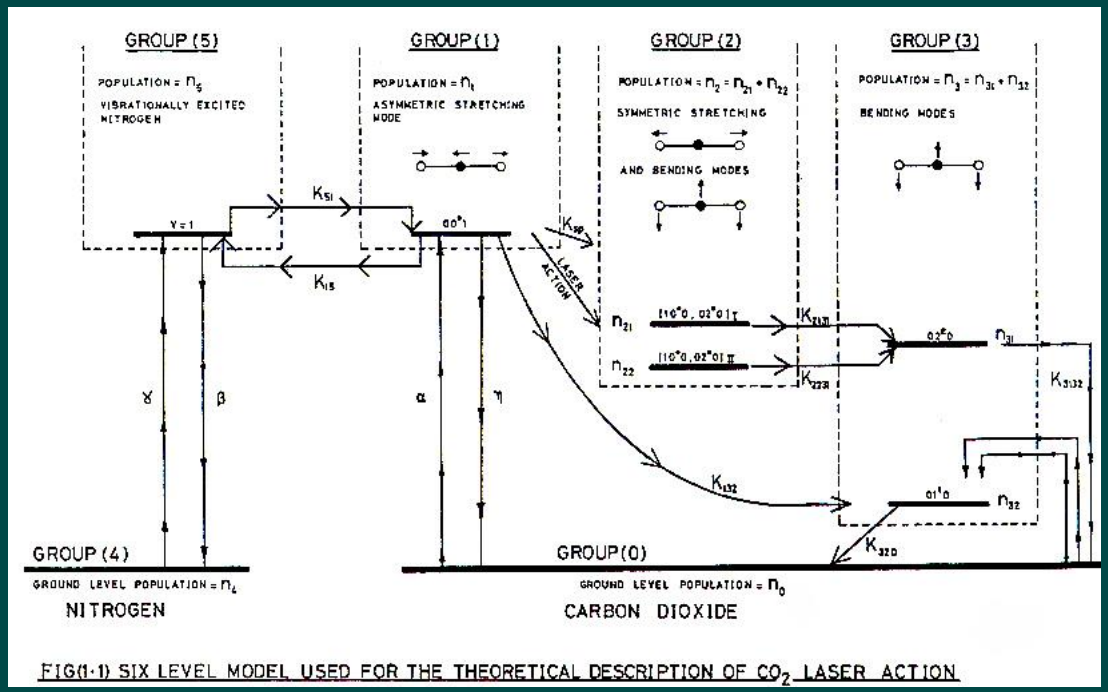

FIG(1·1) SIX LEVEL MODEL USED FOR THE THEORETICAL DESCRIPTION OF CO_2 LASER ACTION

Predicted Laser Output

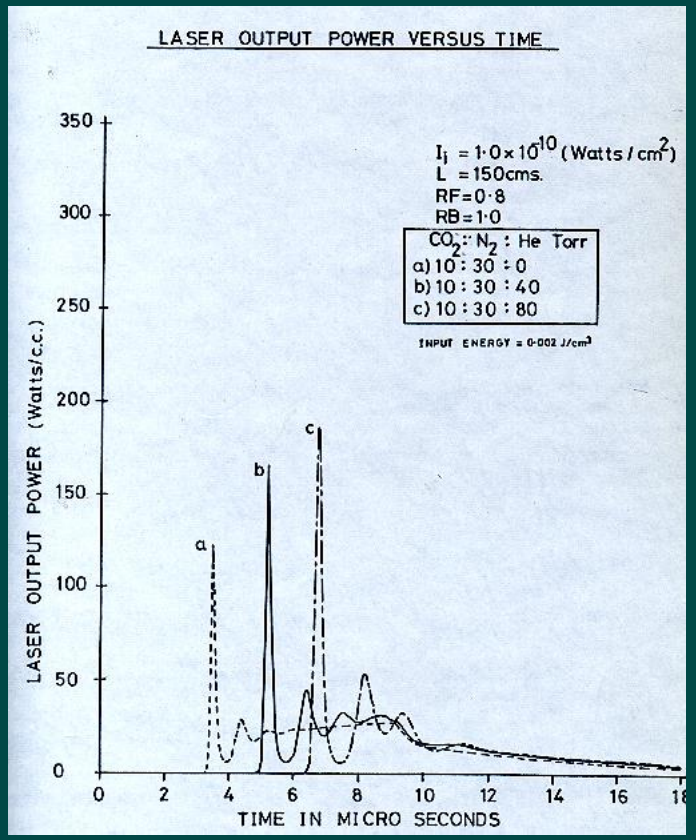

- Optical resonator design
- Output coupling
- Electrical pulse shaping
- Injection of radiation for pulse shape control
- Gas mixture

Second Prototype with Transverse Gas Flow

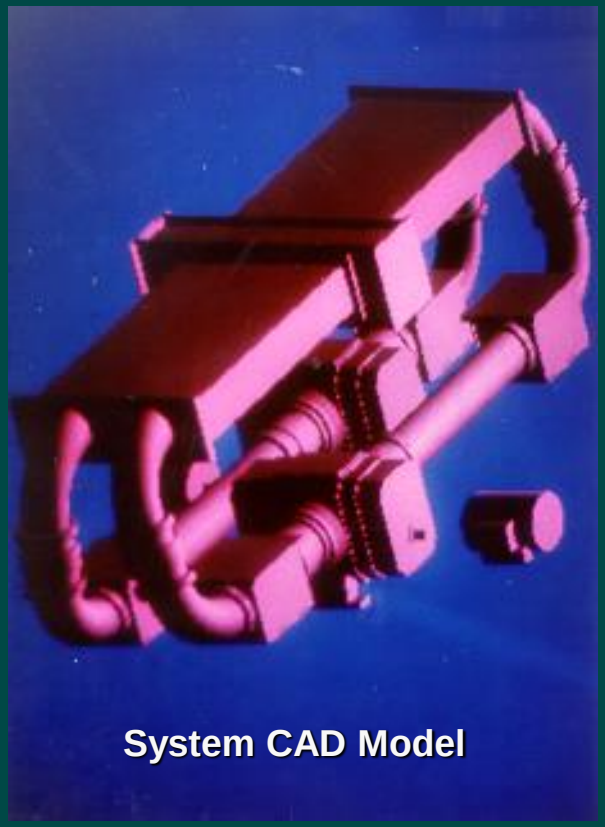

System CAD Model

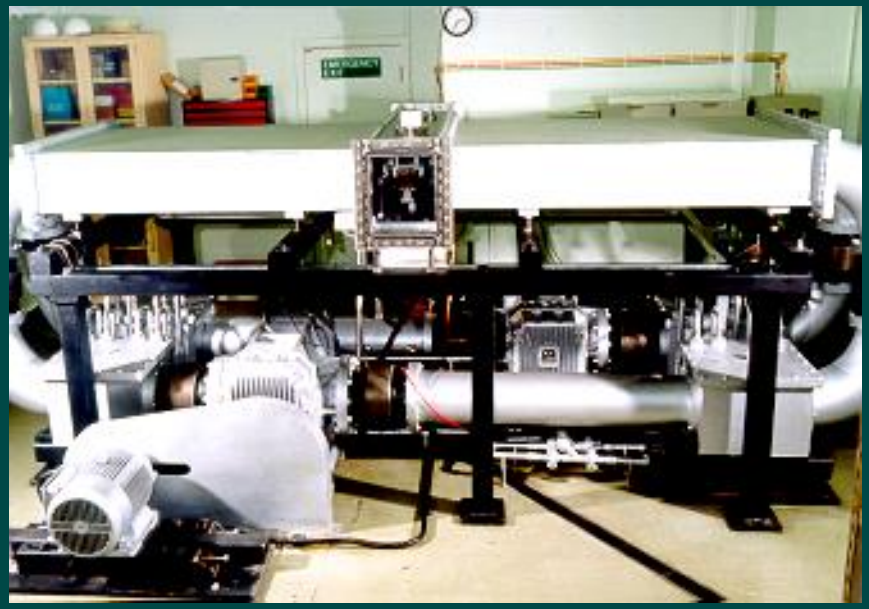

Maximum flow rate - 15,000 m^3/hr
Maximum laser cavity velocity @ 200 Torr - 104 m/s
Cooling capacity 120kW
Laser cavity length 1 metre, Area - 0.04 m^2

Laser Pulsed Power Supply

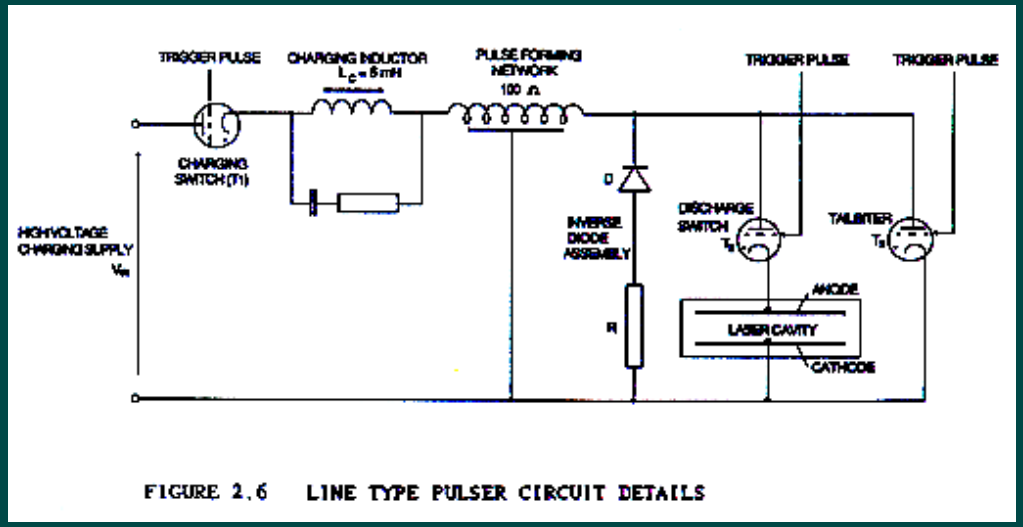

FIGURE 2.6 LINE TYPE PULSER CIRCUIT DETAILS

PRF continuously variable up to - 10 kHz
Peak PFN voltage - 20kV
Maximum pulse duration - 10 μs
Maximum pulse energy - 10 J
Peak pulse voltage - 10 kV
Maximum pulse power - 1 MW

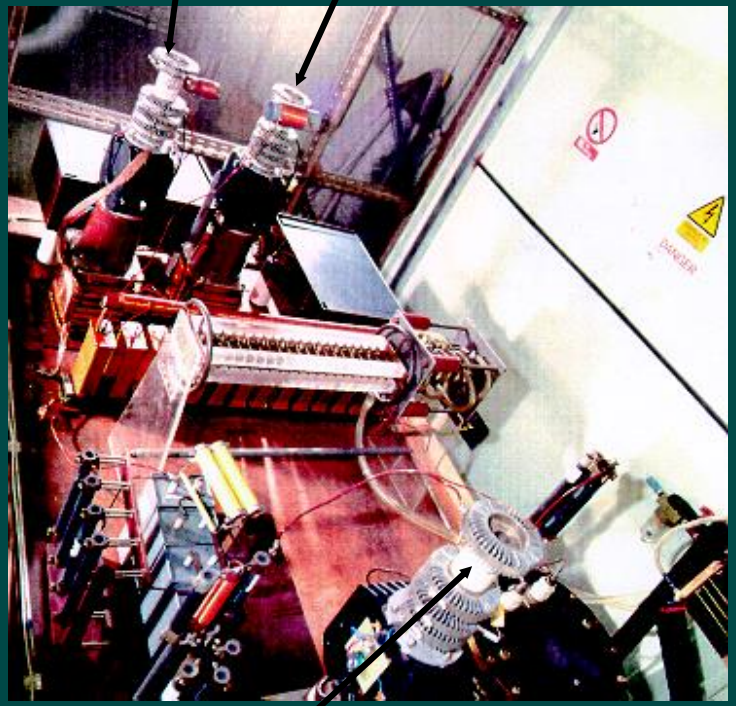

Laser Output Pulse

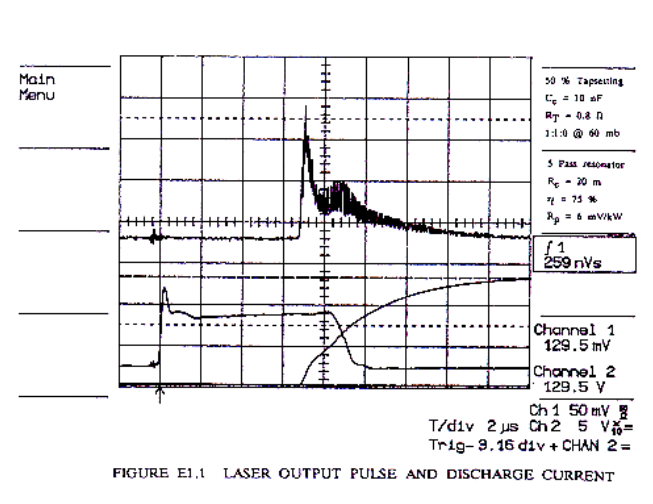

FIGURE E1.1 LASER OUTPUT PULSE AND DISCHARGE CURRENT

Typical output pulse

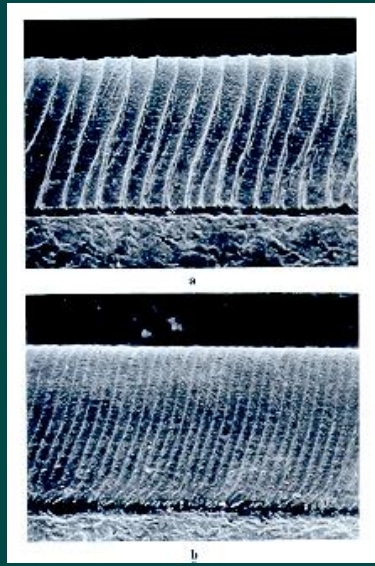

CW laser cutting 1.25 mm thick steel. Mean power 300 W

Pulsed laser cutting

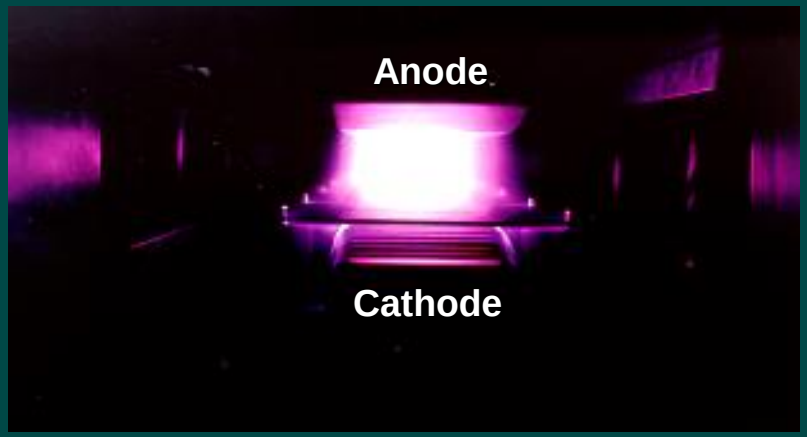

Typical Glow Discharge

Operated at 5 kHz,
Mean power 2 kW,
Pulse power 65 kW

To get to 10 kHz at 5 kW the Trigger Wire Pre-ionisation scheme needed to be replaced with Electron Beam Pre-ionisation. This would give 100 kW pulses

3.5kW Diffusion Cooled CO_2 Laser - CW or 5kHz pulsed

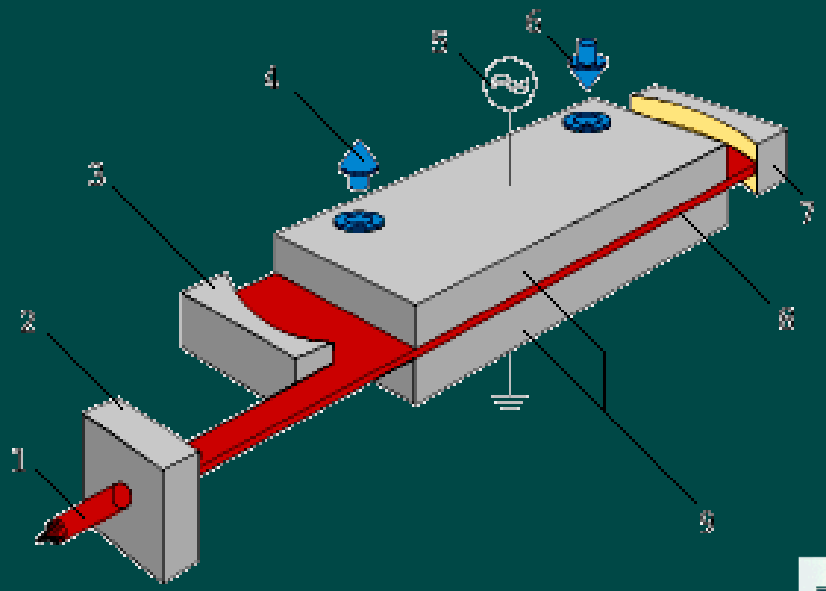

1. Laserbeam
2. Beam shaping unit
3. Output mirror
4. Cooling water
5. RF excitation
6. Cooling water
7. Rear mirror
8. RF excited discharge
9. Waveguiding electrodes

Courtesy of Rofin

Flash Lamp Pumped 2.7kW cw or Pulsed (500 Hz) Nd-YAG Laser

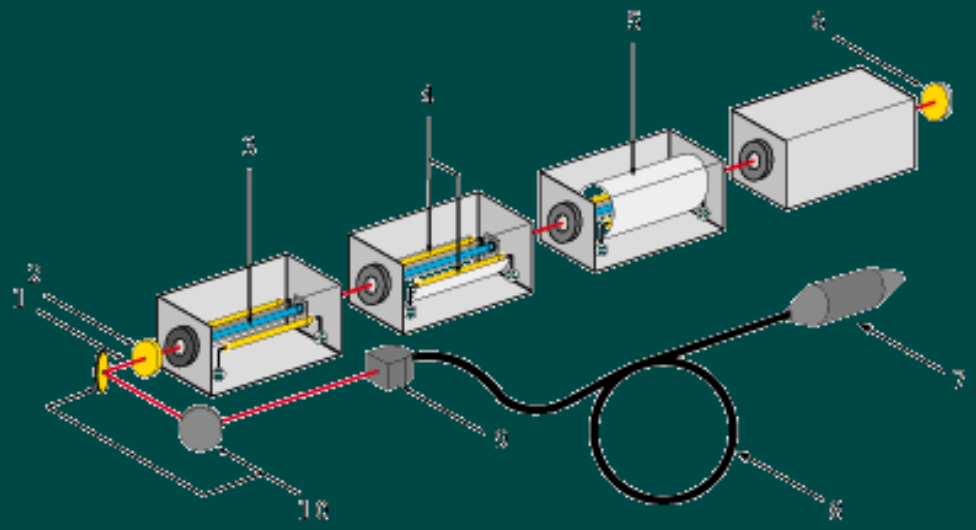

1. Laser beam
2. Output mirror
3. Nd:YAG rod
4. Excitation lamps
5. Reflector
6. Rear mirror
7. Focusing unit
8. Fibre - 600 microns
9. In-coupling unit
10. Beam bending mirrors

Courtesy of Rofin

4.4 kW cw Diode Pumped Nd-YAG Laser

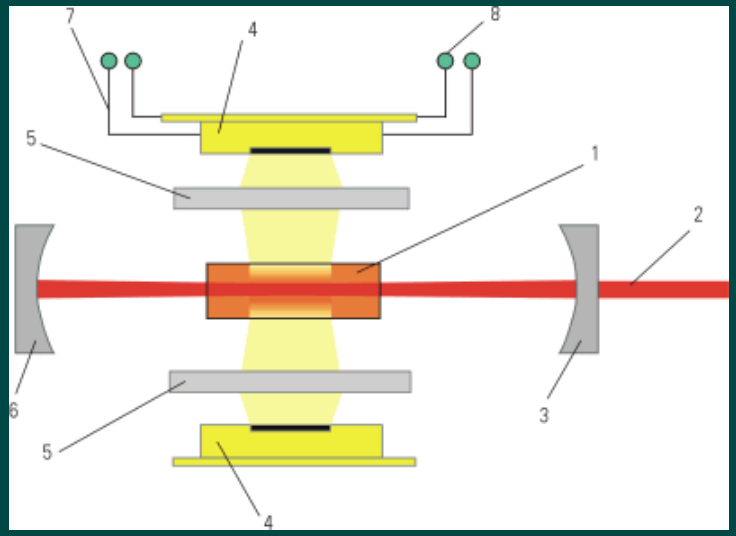

1. Nd:YAG rod
2. Laserbeam
3. Output coupler
4. Diode arrays
5. Collimating optic
6. High-refelectance mirror
7. Cooling
8. Electrical supply

9. 300 micron fibre

Courtesy of Rofin

Long Pulse Interaction

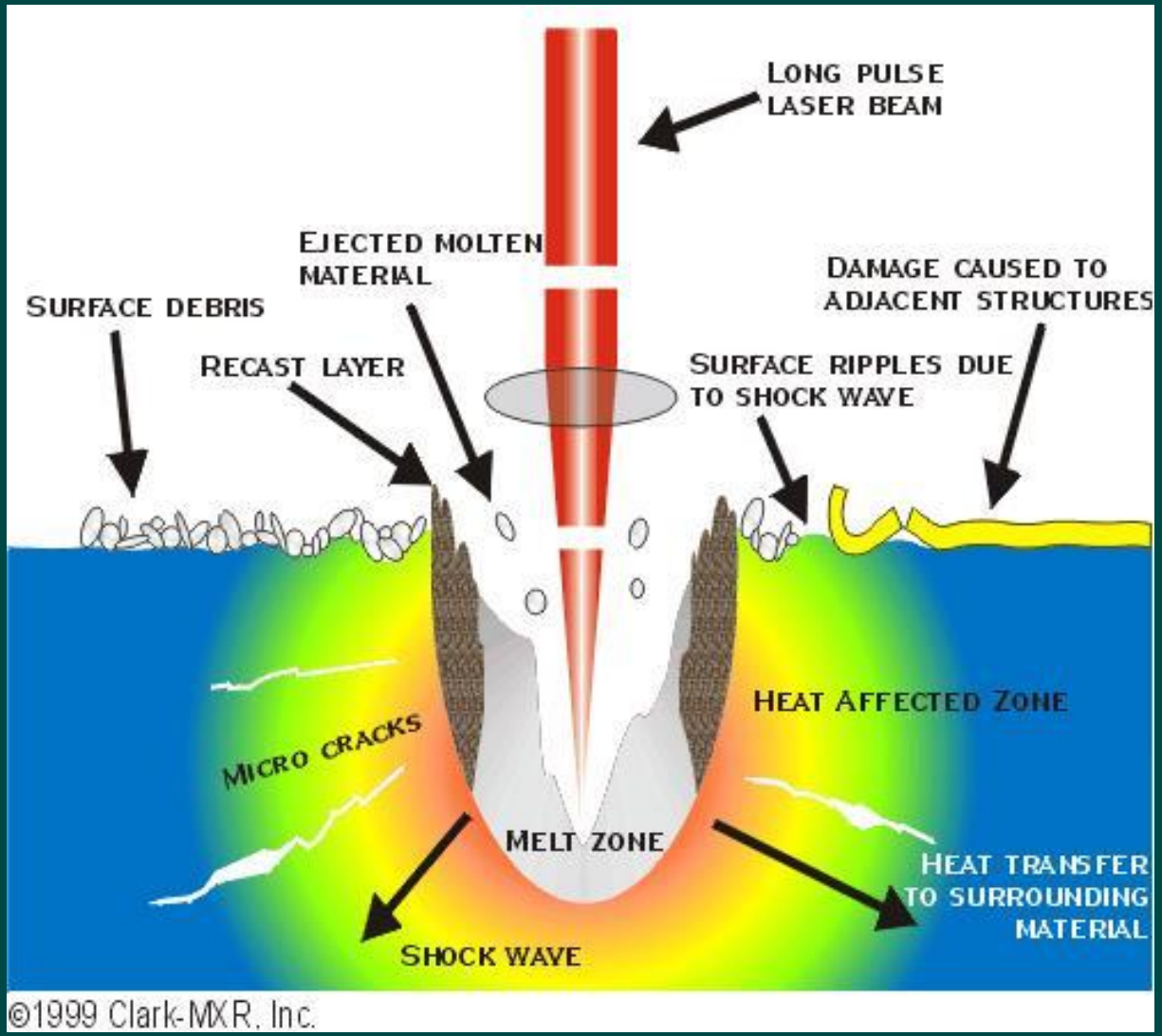

Nd: Glass Laser Interactions

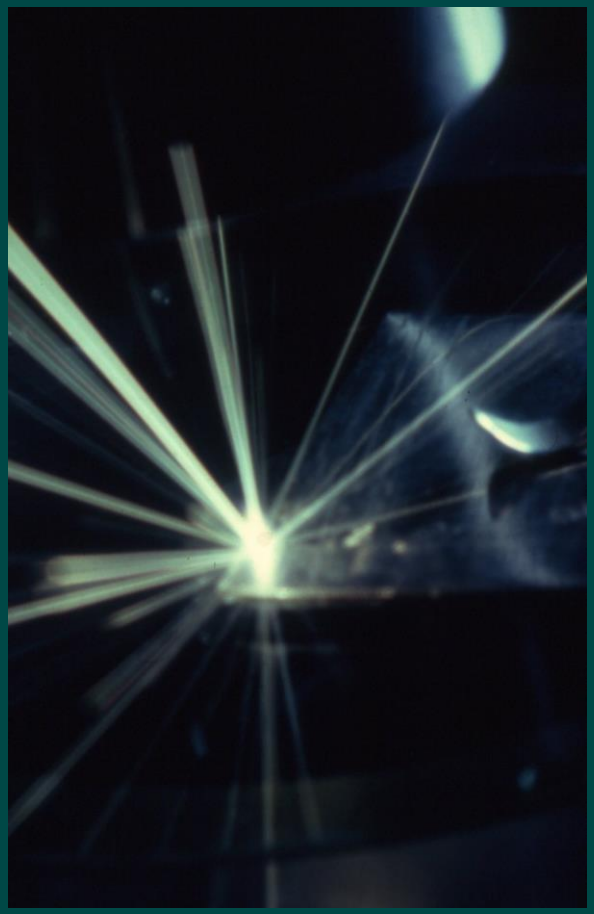

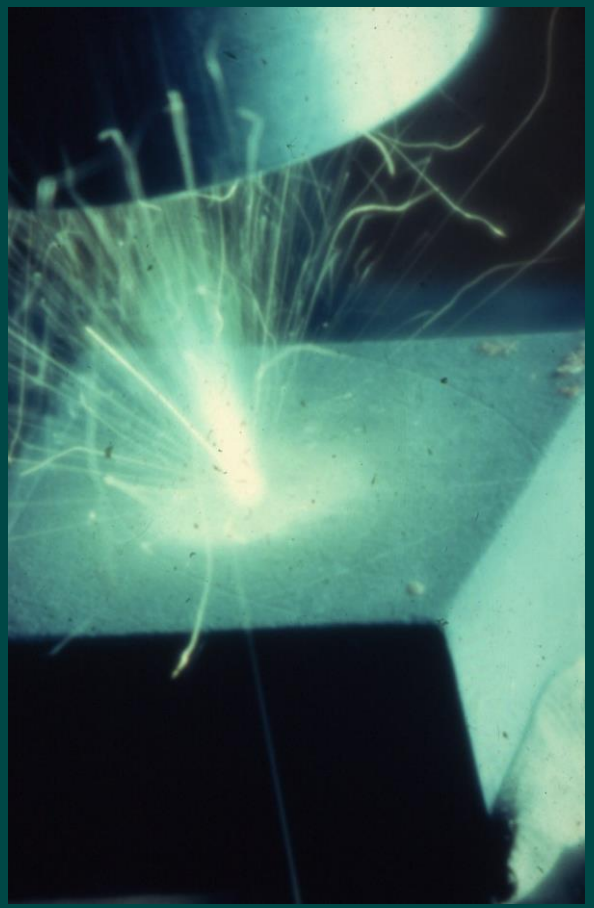

Nd: Glass Laser Interactions

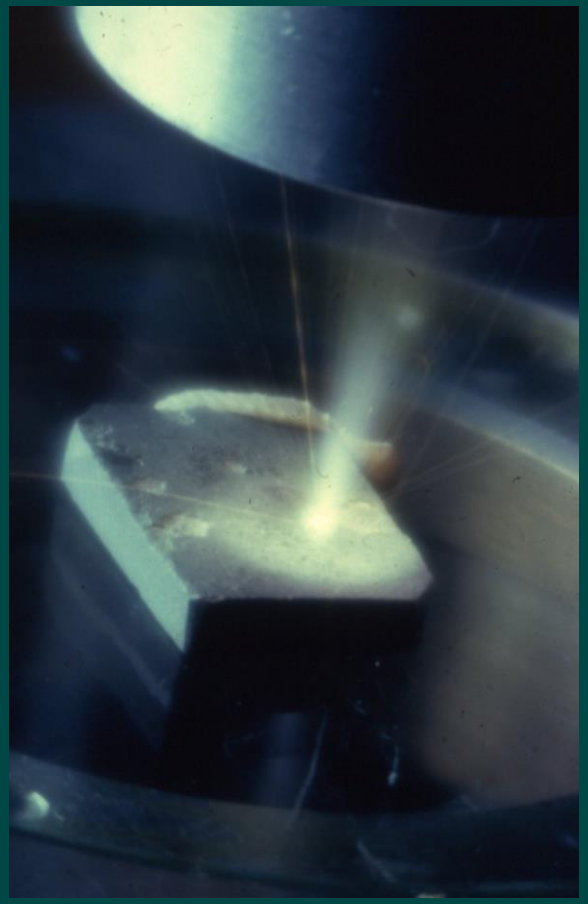

Streak Photographs of Laser Drilling with an Nd:Glass Laser

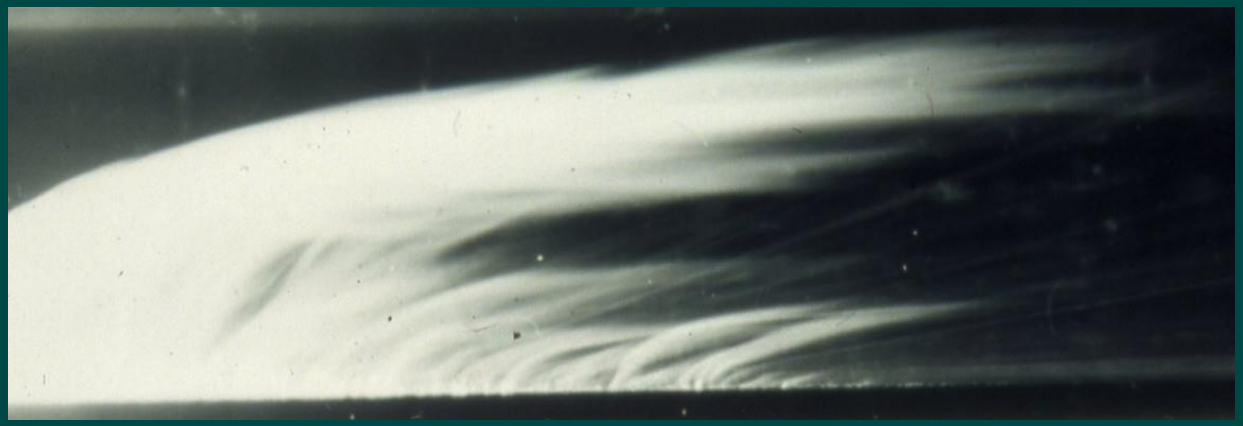

Schematic illustrating electron movement inside metals

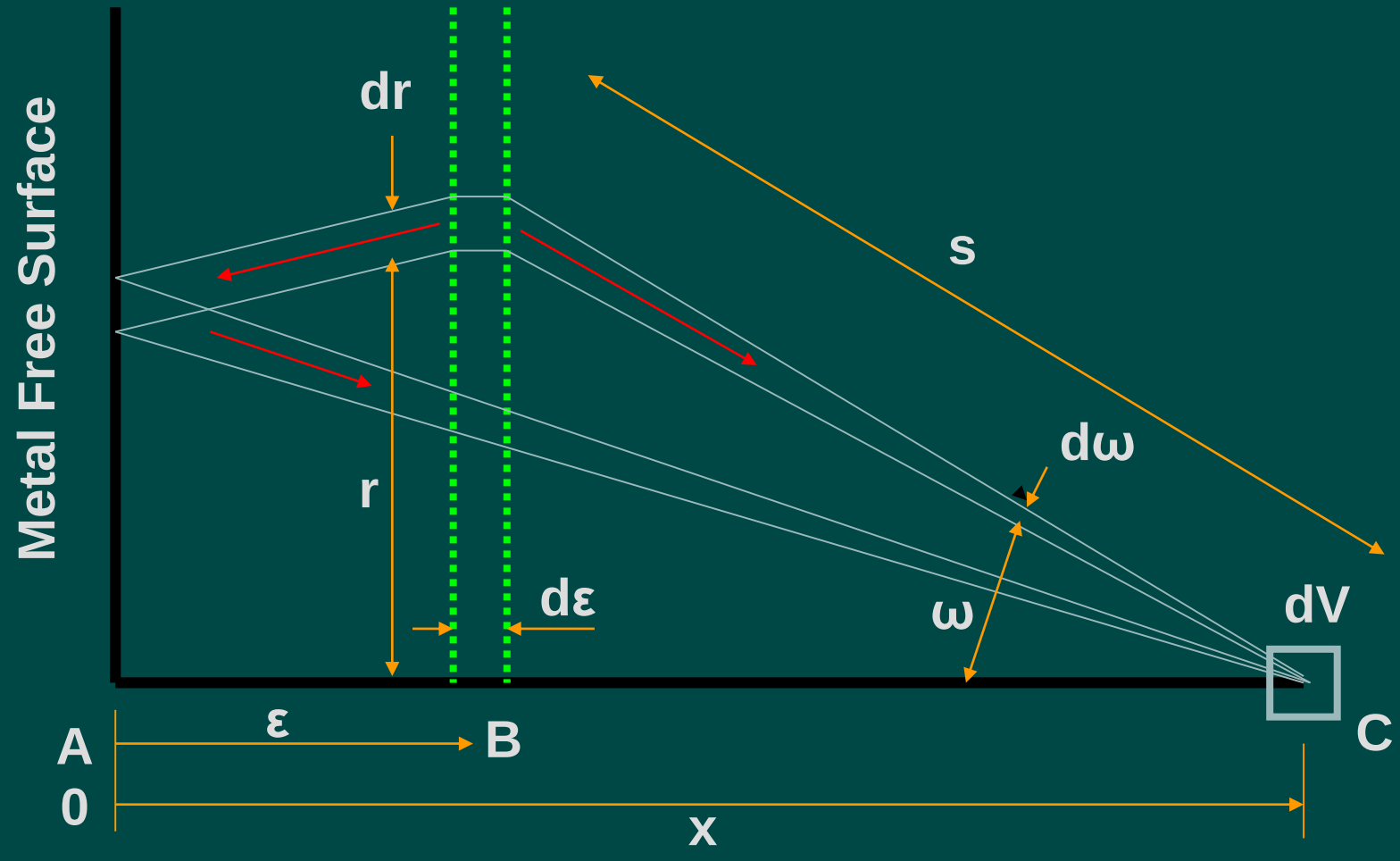

Electron kinematics

- We need to evaluate the number of electrons which leave element ‘dε’ after colliding there
- Then suffer their next collision in a volume element ‘dV’ a distance ‘s’ away in time ‘dt’
- The solid conical element subtends an angle ‘ω’ with the ‘x’ axis.

Electron kinematics

- We need to take account of electrons coming from the right of ‘dV’ and electrons that are reflected from the surface and travel along the path BAC
- To achieve this we can use a mirror image method as shown in the following figure

Schematic illustrating electron movement inside metals using a mirror image method

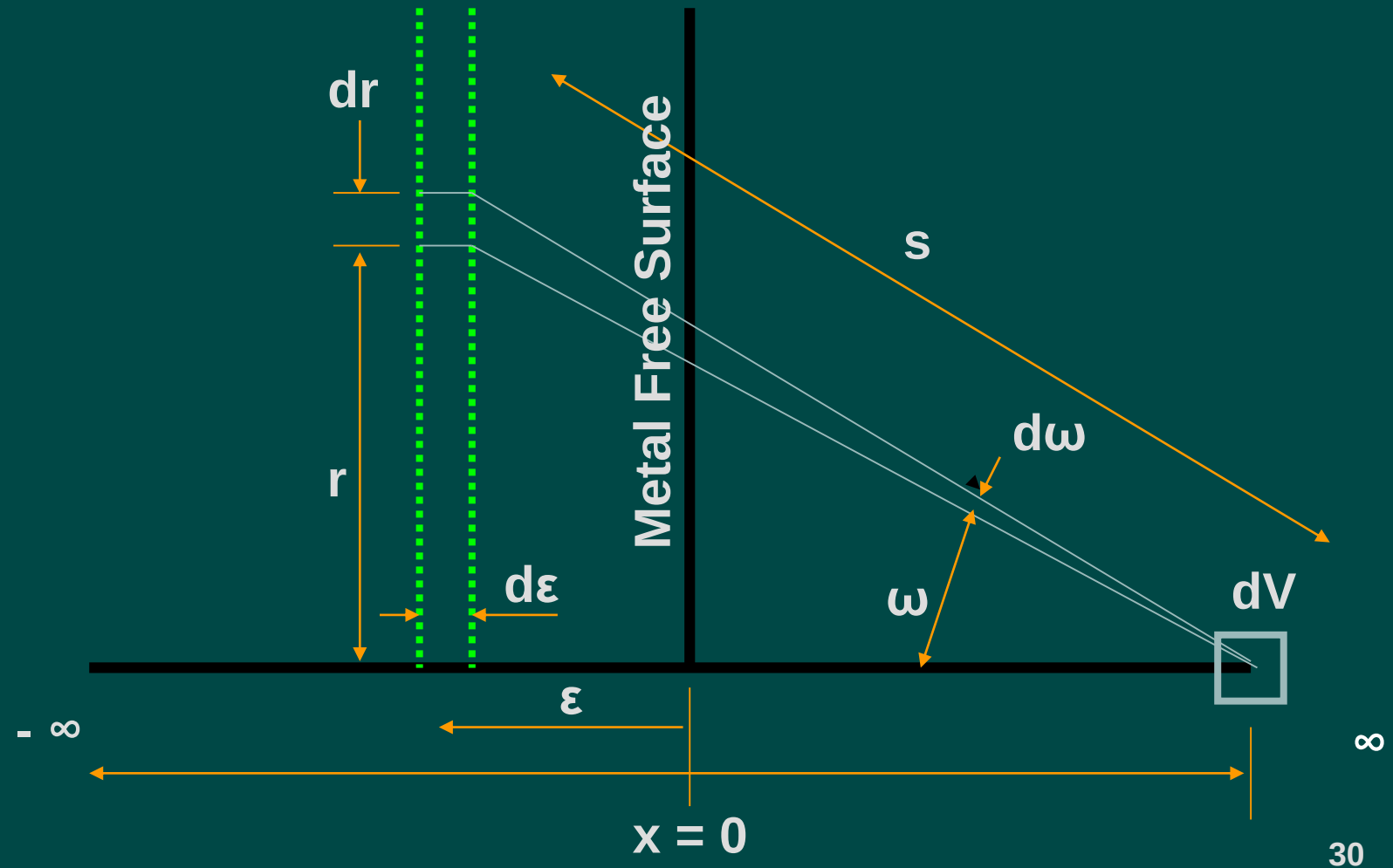

Electrons transported into dV

- Using the mirror image method we must determine the energy transported into ‘dV’ from all electrons in ‘dε’ at ‘ε’

$$n_{\varepsilon V} = \frac{N' z.r d\omega}{2s} e^{(-s/\lambda)} \frac{d\varepsilon.dV}{\lambda \cos\omega} \qquad (1)$$

- N’ = number of Fermi surface electrons; λ = electron-phonon mean free path; z = collision frequency in dV; v = Fermi electron velocity; z = v / λ
- Hence to evaluate the number of electrons arriving in dV which come from dε we must integrate over ‘$-\infty < \varepsilon < \infty$’ and ‘$0 < \omega < \pi/2$’

Energy Transported by Electrons into dV

- The energy carried into the volume dV in time dt by electrons depends upon the specific time at which the electron free path was generated. There are two groups:

  i. *Those travelling a distance $s < vdt$. Electrons generated within the time interval dt will arrive in dV during the same time interval.*

  ii. *Those travelling a distance $s \geq vdt$. These electrons must be generated in the previous time intervals if they are to arrive in dV during the current dt.*

Energy Transported by Electrons into dV

- Therefore the average energy E stored in the electron at ε is:

$$E = E(\varepsilon,t) + \frac{1}{2}\left\{dt - \frac{2|s|}{v}\right\}\frac{\partial E(\varepsilon,t)}{\partial t} \qquad (2)$$

Schematic to show the photon absorption process from ε to x

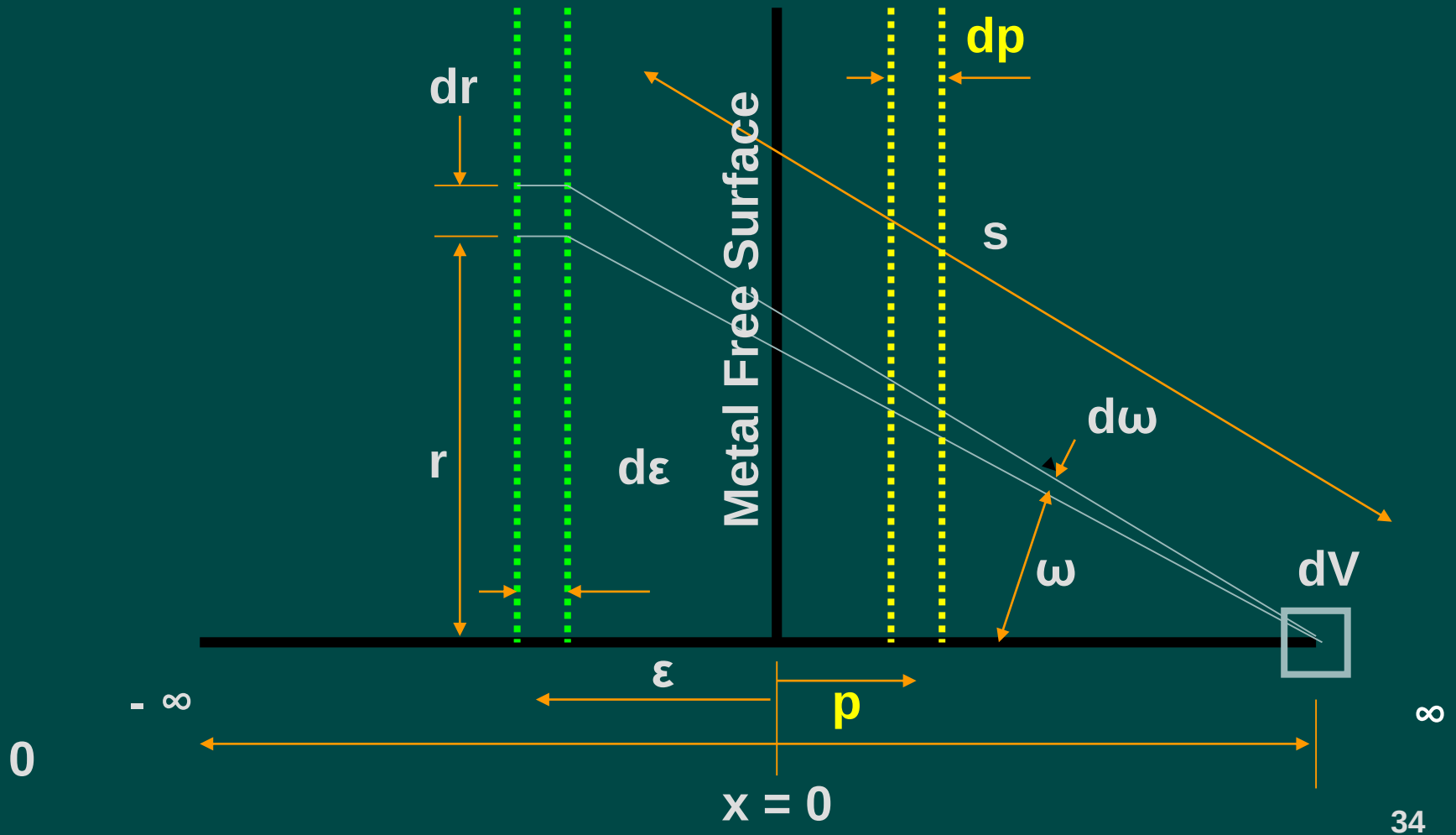

Photon Absorption

- Ignoring quantum effects, free electrons are assumed to acquire the laser energy by merely passing through the electromagnetic field of the incident beam
- The field is described by Lamberts law:

$$I(x,t) = I_0(1-R(t))e^{(-\delta x)} \qquad (3)$$

- I(x,t) is the beam intensity at time t after propagating distance x in the material. $I_0(t)$ is the intensity at the surface. R(t) is the reflection coefficient and δ is the absorption coefficient

Photon absorption by electrons

- Considering the small element dp; the power absorbed per unit area by electrons at time t is:

$$I_0(t)(1-R(t))\delta e^{(-\delta p)}dp \qquad (4)$$

- The energy absorbed per electron is:

$$\frac{I_0(t)(1-R(t))\delta e^{(-\delta p)}dp\Delta t}{N'} \qquad (5)$$

- Where Δt is the average time an electron stays in the element dp; $\Delta t = dp / v\cos\omega$ (6)

Photon absorption by electrons

- It can be assumed that $I_0(t)$ and $R(t)$ are constants in the time required for the electrons to move from ε to x
- Hence, substituting for Δt and integrating. The energy absorbed per electron in moving from ε to x is:

$$\frac{I_0(1-R)\delta}{N'\nu\cos\omega}\left|\int_{\varepsilon}^{x} e^{(-\delta p)}dp\right| \qquad (7)$$

Average energy of arriving electrons

- From (2) and (7) the average energy of an electron entering dV at x from ε after dt is:

$$E(\varepsilon,t)+\frac{1}{2}\left\{dt-\frac{2|s|}{v}\right\}\frac{\partial E(\varepsilon,t)}{\partial t}+\frac{I_0(1-R)\delta}{N'v\cos\omega}\left|\int_{\varepsilon}^{x}e^{(-\delta p)}dp\right| \qquad (8)$$

- If $E_p(x,t)$ is the average energy of phonons in dV at x, the energy given up by electrons to the phonons on collision is:

  $f\{E(x, t+dt) - E_p(x,t)\}$ (9)

  Where f is the fraction of the energy difference between an electron and a phonon given up by an electron on collision with a phonon

The rate at which electrons loose energy to phonons in elastic collisions

- The fraction f of the average energy difference between electrons and the lattice in any given volume is:

$$f(x,t) = \frac{8m}{3M}\left\{1 - \frac{T(x,t)}{T_e(x,t)}\right\}$$

- Where m and M are the masses of the electrons and lattice atoms respectively, $T_e(x,t)$ and $T(x,t)$ are their temperatures at time t and distance x.

Energy of the Lattice Phonons

- The total energy transferred to the lattice from all electrons colliding in dV at x over the time interval dt is equal to the energy increase of the lattice, where n(x,t) is the number density of atoms:

$$\frac{\partial n E_p(x,t)}{\partial t} dV =$$

$$dV \int_{-\infty}^{\infty} \int_{0}^{\pi/2} \left\{ \frac{N'\nu}{2\lambda} . e^{(-|x-\varepsilon|/\lambda \cos\omega)} \frac{\sin\omega}{\lambda \cos\omega} \right\}$$

$$\times (f) \times \left\{ E(\varepsilon,t) + \frac{1}{2} \left\{ dt - \frac{2|s|}{\nu} \right\} \frac{\partial E(\varepsilon,t)}{\partial t} + \frac{I_0(1-R)\delta}{N'\nu \cos\omega} \left| \int_{\varepsilon}^{x} e^{(-\delta p)} dp \right| - E_p(x,t) \right\} d\omega d\varepsilon \qquad (10)$$

Energy of the Electrons

- The average energy change of electrons at x equals the energy left in the electrons after collision less the energy carried away by electrons leaving the elemental volume dV during dt

$$\frac{\partial N' E(x,t)}{\partial t} dV =$$

$$dV \int_{-\infty}^{\infty} \int_{0}^{\pi/2} \left\{ \frac{N'\nu}{2\lambda} . e^{(-|x-\varepsilon|/\lambda\cos\omega)} \frac{\sin\omega}{\lambda\cos\omega} \right\} \times \left\{ E(\varepsilon,t) + \frac{1}{2} \left\{ dt - \frac{2|s|}{\nu} \right\} \frac{\partial E(\varepsilon,t)}{\partial t} + \frac{I_0(1-R)\delta}{N'\nu\cos\omega} \left| \int_{\varepsilon}^{x} e^{(-\delta p)} dp \right| \right\} d\omega d\varepsilon$$

$$-dV \frac{\partial n E_p(x,t)}{\partial t} - dV \frac{N'\nu}{\lambda} E(x,t) \qquad (11)$$

Continuity equation for electrons

$$\frac{\partial N'(x,t)}{\partial t} = \int_{-\infty}^{\infty}\int_{0}^{\pi/2} \left\{ \frac{N'\nu}{2\lambda^2}.e^{(-|x-\varepsilon|/\lambda\cos\omega)} \frac{\sin\omega}{\cos\omega} \right\} d\omega d\varepsilon - \frac{N'\nu}{\lambda} \qquad (12)$$

Assuming that the electron gas is in a state of equilibrium, the participating electrons can be obtained from the ordinary Fermi distribution function:

$$N' = \frac{NT_e\pi^2}{2T_F} \qquad (13)$$

where T_F is the Fermi temperature, T_e is the electron temperature, N is the number density of valency electrons

Thermal Properties

- The thermal conductivity (K) of the material can be shown to be:

$$K = \frac{N' v \lambda k}{3} \qquad (14)$$

- The heat capacity is:

$$\rho \, C_p = 3nk \qquad (15)$$

- Where k is the Boltzmann constant, ρ is the material density, C_p is the specific heat and n is the phonon atoms number density

Expressing the equations in terms of electron and phonon temperature - Lattice

- Using equations (13), (14) and (15) in (10), (11) and (12)

$$\frac{\partial}{\partial t}[\rho C_p T] =$$

$$f \int_{-\infty}^{\infty} \frac{9K}{4\lambda^3} \int_{0}^{\pi/2} \left\{ e^{(-|x-\varepsilon|/\lambda\cos\omega)} \frac{\sin\omega}{\cos\omega} \right\} \times \left\{ T_e(\varepsilon,t) + \frac{1}{2} \left\{ dt - \frac{2|s|}{v} \right\} \frac{\partial T_e(\varepsilon,t)}{\partial t} - T(x,t) \right\} d\omega d\varepsilon$$

$$+ f \frac{I_0(1-R)\delta}{2\lambda^2} \int_{-\infty}^{\infty} \int_{0}^{\pi/2} \left\{ e^{(-|x-\varepsilon|/\lambda\cos\omega)} \frac{\sin\omega}{\cos^2\omega} \right\} \left| \int_{\varepsilon}^{x} e^{(-\delta p)} dp \right| d\omega d\varepsilon \qquad (16)$$

Expressing the equations in terms of electron and phonon temperature - Electrons

$$\frac{\partial}{\partial t}\left\{\frac{9KT_e}{2\lambda v}\right\} = (1-f)\int_{-\infty}^{\infty}\frac{9K}{4\lambda^3}\int_{0}^{\pi/2}\left\{e^{(-|x-\varepsilon|/\lambda\cos\omega)}\frac{\sin\omega}{\cos\omega}\right\}\times\left\{T_e(\varepsilon,t)+\frac{1}{2}\left\{dt-\frac{2|s|}{v}\right\}\frac{\partial T_e(\varepsilon,t)}{\partial t}\right.d\omega d\varepsilon$$

$$+ f\int_{-\infty}^{\infty}\frac{9K}{4\lambda^3}\int_{0}^{\pi/2}\left\{e^{(-|x-\varepsilon|/\lambda\cos\omega)}\frac{\sin\omega}{\cos\omega}\right\}T(\varepsilon,t)d\omega d\varepsilon$$

$$+ f\frac{I_0(1-R)\delta}{2\lambda^2}\int_{-\infty}^{\infty}\int_{0}^{\pi/2}\left\{e^{(-|x-\varepsilon|/\lambda\cos\omega)}\frac{\sin\omega}{\cos^2\omega}\right\}\left|\int_{\varepsilon}^{x}e^{(-\delta p)}dp\right|d\omega d\varepsilon - \frac{9K}{2\lambda^2}T_e(x,t)$$

(17)

Electron Continuity Equation

$$\frac{\partial K}{\partial t} = \int_{-\infty}^{\infty} \int_{0}^{\pi/2} \left\{ \frac{K\nu}{2\lambda^2} . e^{(-|x-\varepsilon|/\lambda \cos\omega)} \frac{\sin\omega}{\cos\omega} \right\} d\omega d\varepsilon - \frac{K\nu}{\lambda} \qquad (18)$$

Schematic illustrating electron movement inside metals, the material is moving with velocity V_s

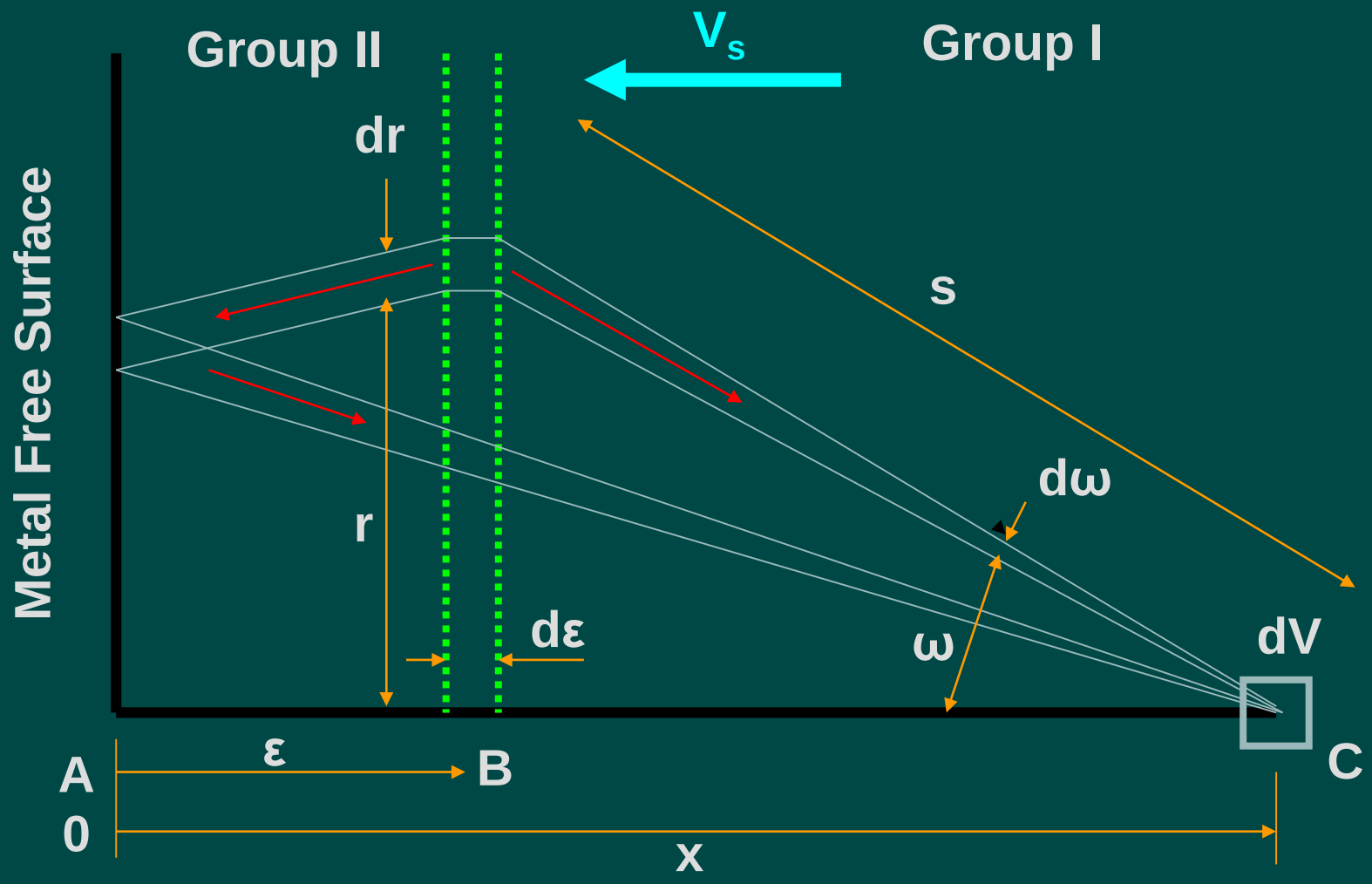

Schematic of one dimensional moving boundary problem

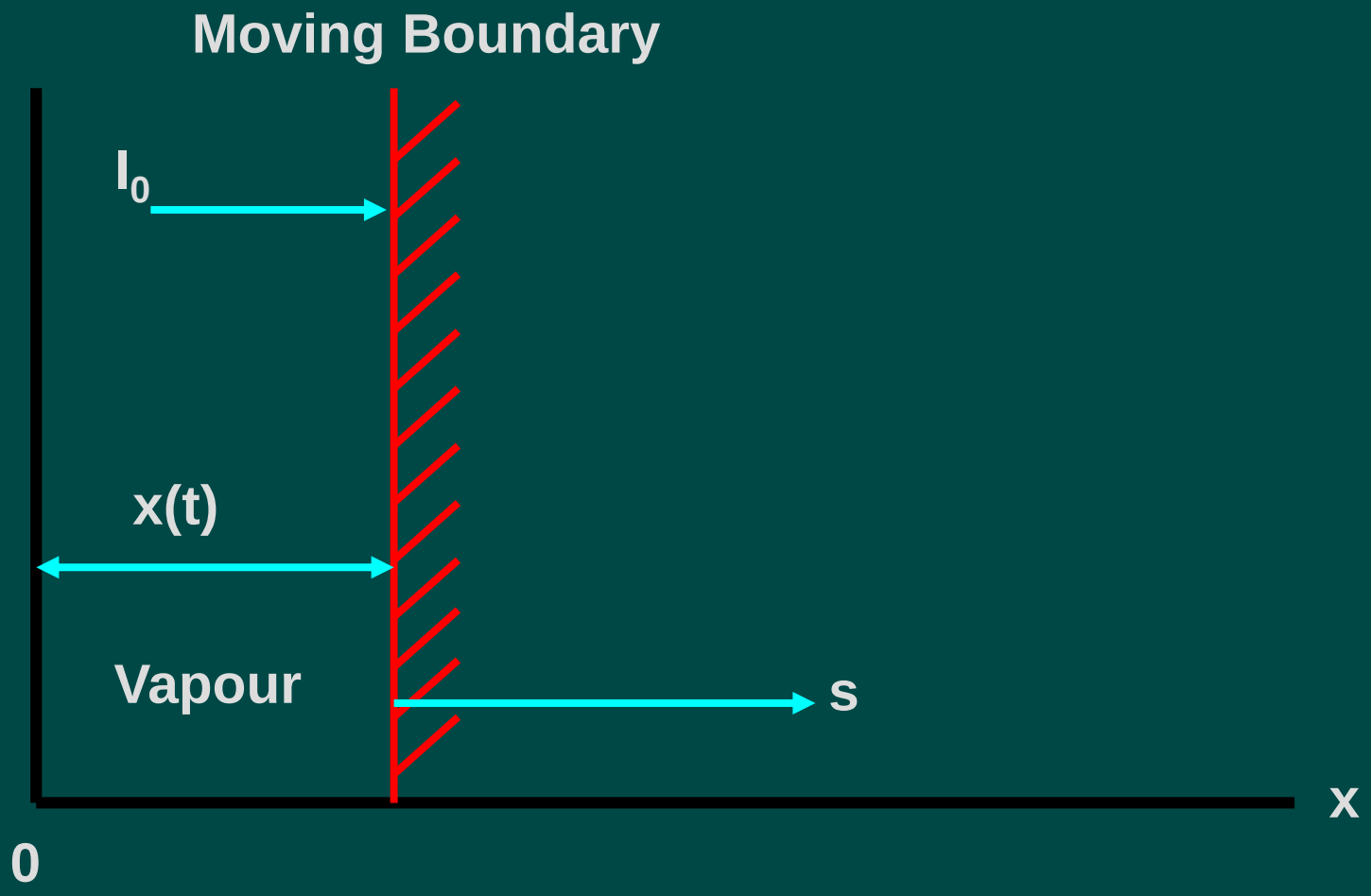

Incorporating Evaporation

- The evaporation rate is given by:

$$G = n\sqrt{\left\{\frac{kT}{2\pi m}\right\}}.e^{-U_0/kT_s} \qquad (19)$$

- Where: n = the atom number density at the surface,
- m = mass of the atom, U_0 = latent heat of vaporisation per atom. The velocity of the evaporating surface V_s is given by:

$$G = V_s = n\sqrt{\left\{\frac{kT}{2\pi m}\right\}}.e^{-U_0/kT_s} \qquad (20)$$

Incorporating Evaporation

- At the surface there is a mathematical singularity, this can be handled by changing the coordinate system such that the material moves with velocity V_s towards the origin.
- The problem is then to determine the energy transported into dV at x from all electrons in dε at ε, then integrate for ε to allow for contributions from the whole of the material, bearing in mind that the bulk material is moving through the coordinate system with velocity V_s

Incorporating Evaporation

- As $V_s << v$ we can neglect the effect of material movement on electron transport.
- The convective heat transfer due to the moving material alters the equations describing the lattice and electron energy distributions

Incorporating Evaporation - Lattice

$$\frac{\partial}{\partial t}[\rho C_p T] - V_s \frac{\partial}{\partial x}[\rho C_p T] =$$

$$f \int_{-\infty}^{\infty} \frac{9K}{4\lambda^3} \int_0^{\pi/2} \left\{ e^{(-|x-\varepsilon|/\lambda\cos\omega)} \frac{\sin\omega}{\cos\omega} \right\} \times \left\{ T_e(\varepsilon,t) + \frac{1}{2} \left\{ dt - \frac{2|s|}{v} \right\} \frac{\partial T_e(\varepsilon,t)}{\partial t} - T(x,t) \right\} d\omega d\varepsilon$$

$$+ f \frac{I_0(1-R)\delta}{2\lambda^2} \int_{-\infty}^{\infty} \int_0^{\pi/2} \left\{ e^{(-|x-\varepsilon|/\lambda\cos\omega)} \frac{\sin\omega}{\cos^2\omega} \right\} \left| \int_{\varepsilon}^{x} e^{(-\delta p)} dp \right| d\omega d\varepsilon \qquad (21)$$

- With the evaporation term $\rho L(T_s)V_s$ added at $x = 0$

Incorporating Evaporation - Electrons

$$\frac{\partial}{\partial t}\left\{\frac{9KT_e}{2\lambda v}\right\} = (1-f)\int_{-\infty}^{\infty}\frac{9K}{4\lambda^3}\int_{0}^{\pi/2}\left\{e^{(-|x-\varepsilon|/\lambda\cos\omega)}\frac{\sin\omega}{\cos\omega}\right\}\times\left\{T_e(\varepsilon,t)+\frac{1}{2}\left\{dt-\frac{2|s|}{v}\right\}\frac{\partial T_e(\varepsilon,t)}{\partial t}\right. d\omega d\varepsilon$$

$$+ f\int_{-\infty}^{\infty}\frac{9K}{4\lambda^3}\int_{0}^{\pi/2}\left\{e^{(-|x-\varepsilon|/\lambda\cos\omega)}\frac{\sin\omega}{\cos\omega}\right\}T(\varepsilon,t)d\omega d\varepsilon$$

$$+ f\frac{I_0(1-R)\delta}{2\lambda^2}\int_{-\infty}^{\infty}\int_{0}^{\pi/2}\left\{e^{(-|x-\varepsilon|/\lambda\cos\omega)}\frac{\sin\omega}{\cos^2\omega}\right\}\left|\int_{\varepsilon}^{x}e^{(-\delta p)}dp\right| d\omega d\varepsilon - \frac{9K}{2\lambda^2}T_e(x,t)+V_s\frac{\partial}{\partial x}[\rho C_p T]$$

(22)

Electron Continuity Equation

$$\frac{\partial K}{\partial t} = \int_{-\infty}^{\infty} \int_{0}^{\pi/2} \left\{ \frac{K\nu}{2\lambda^2} . e^{(-|x-\varepsilon|/\lambda \cos\omega)} \frac{\sin\omega}{\cos\omega} \right\} d\omega d\varepsilon - \frac{K\nu}{\lambda} \qquad (23)$$

This gives a system of nonlinear integro-differential equations which are solved using numerical methods

Surface Temperature Variation in Aluminium using the Kinetic Theory

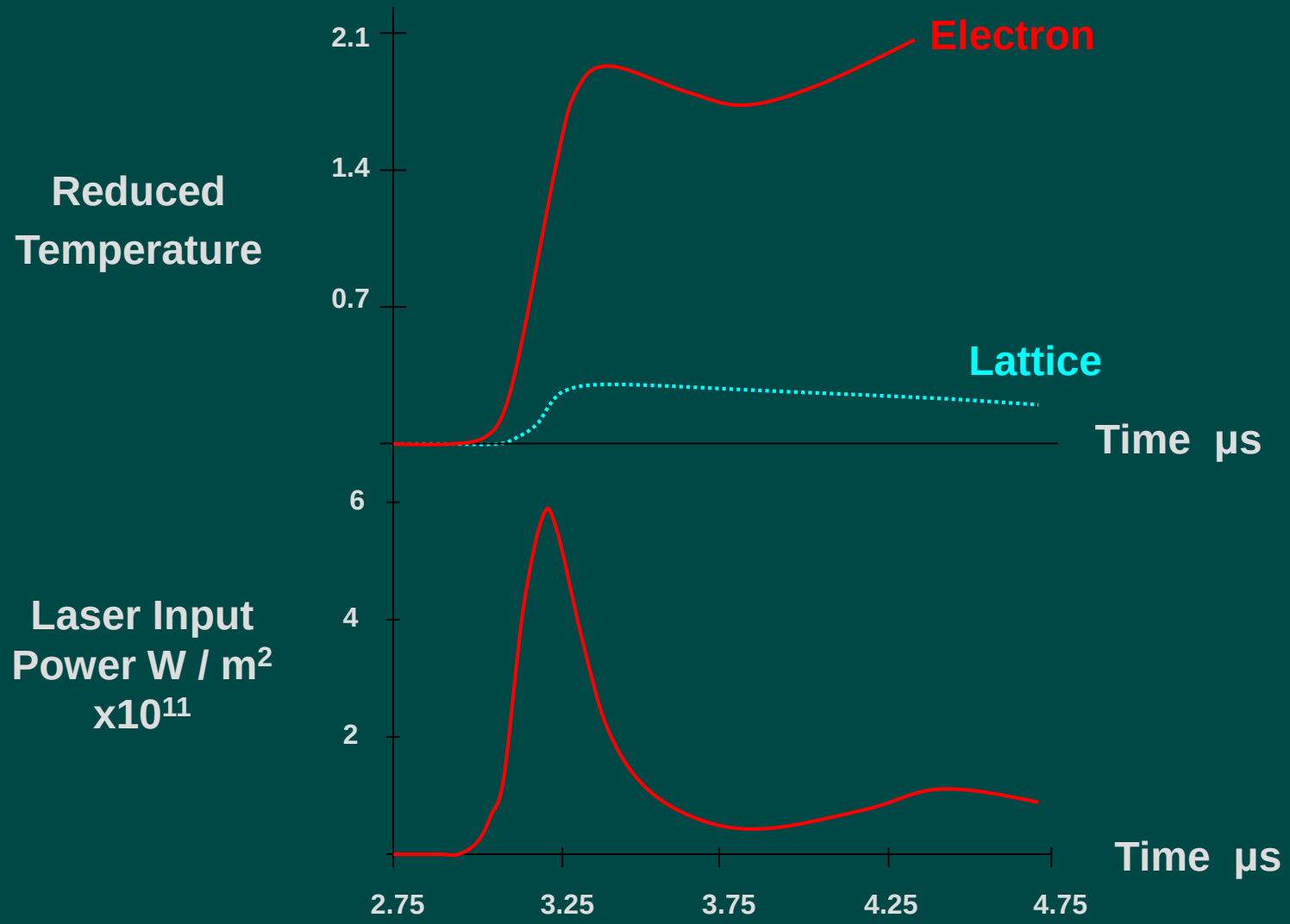

Surface Temperature Variation in Copper using the Kinetic Theory

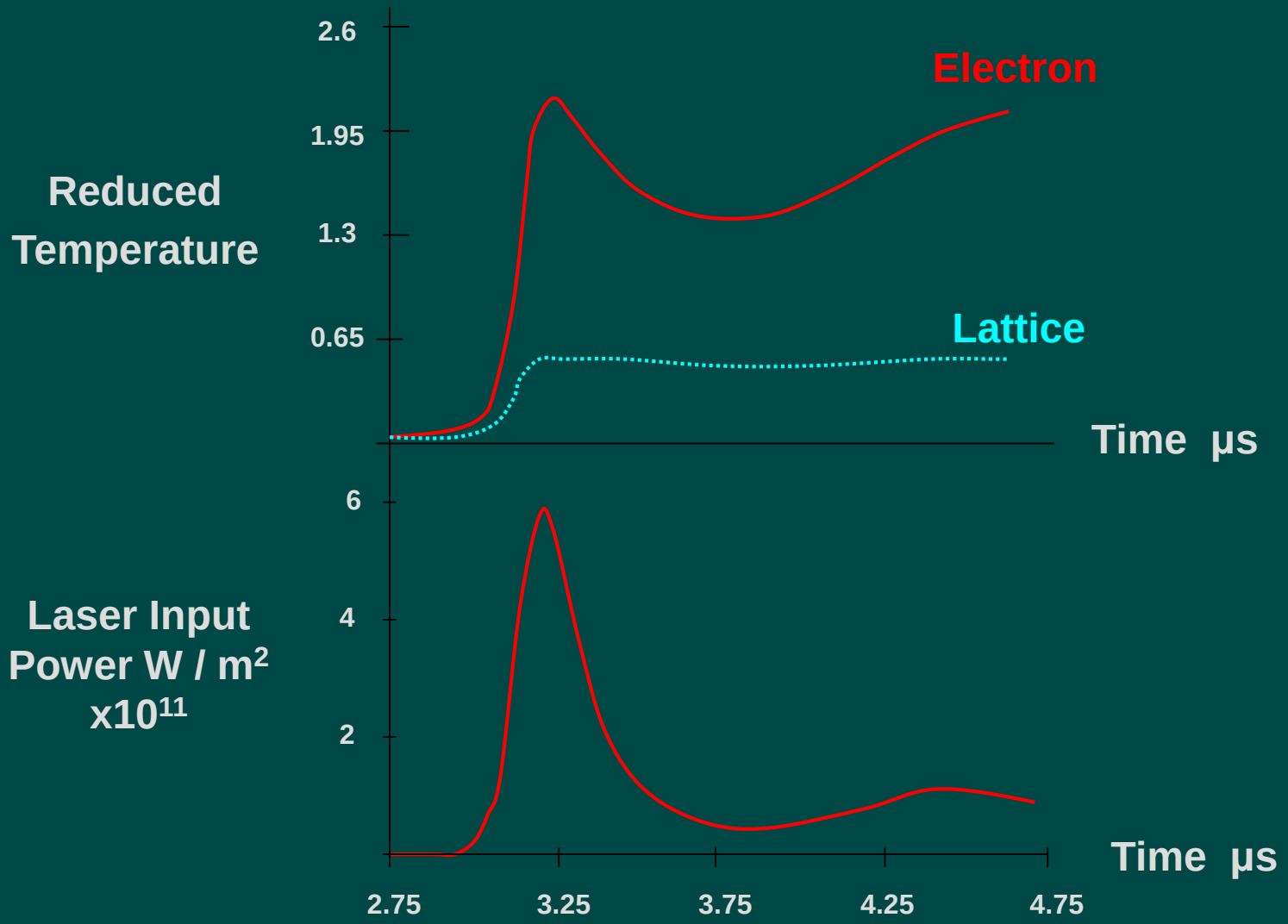

Lattice Temperature Profile in Aluminium

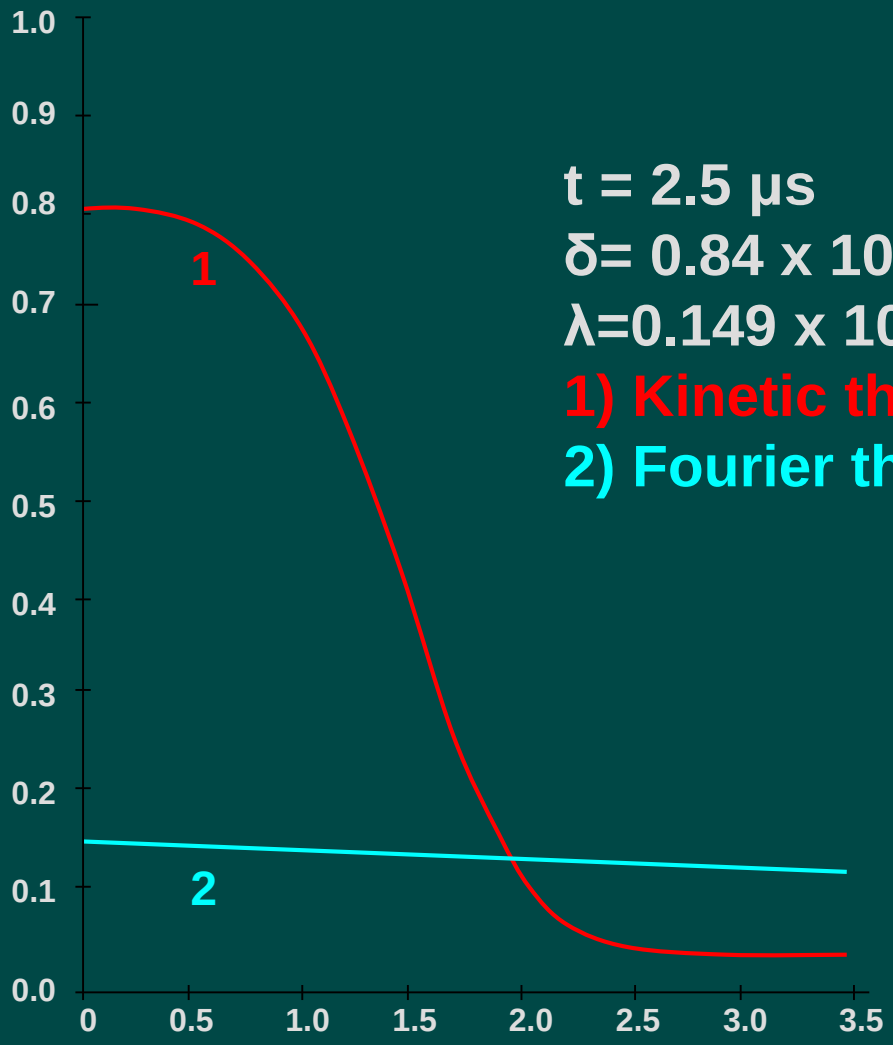

$t = 2.5\ \mu s$

$\delta = 0.84 \times 10^{8}\ m^{-1}$

$\lambda = 0.149 \times 10^{-7} m$

1) Kinetic theory

2) Fourier theory

Temperature Profile in Copper Using the Kinetic Theory

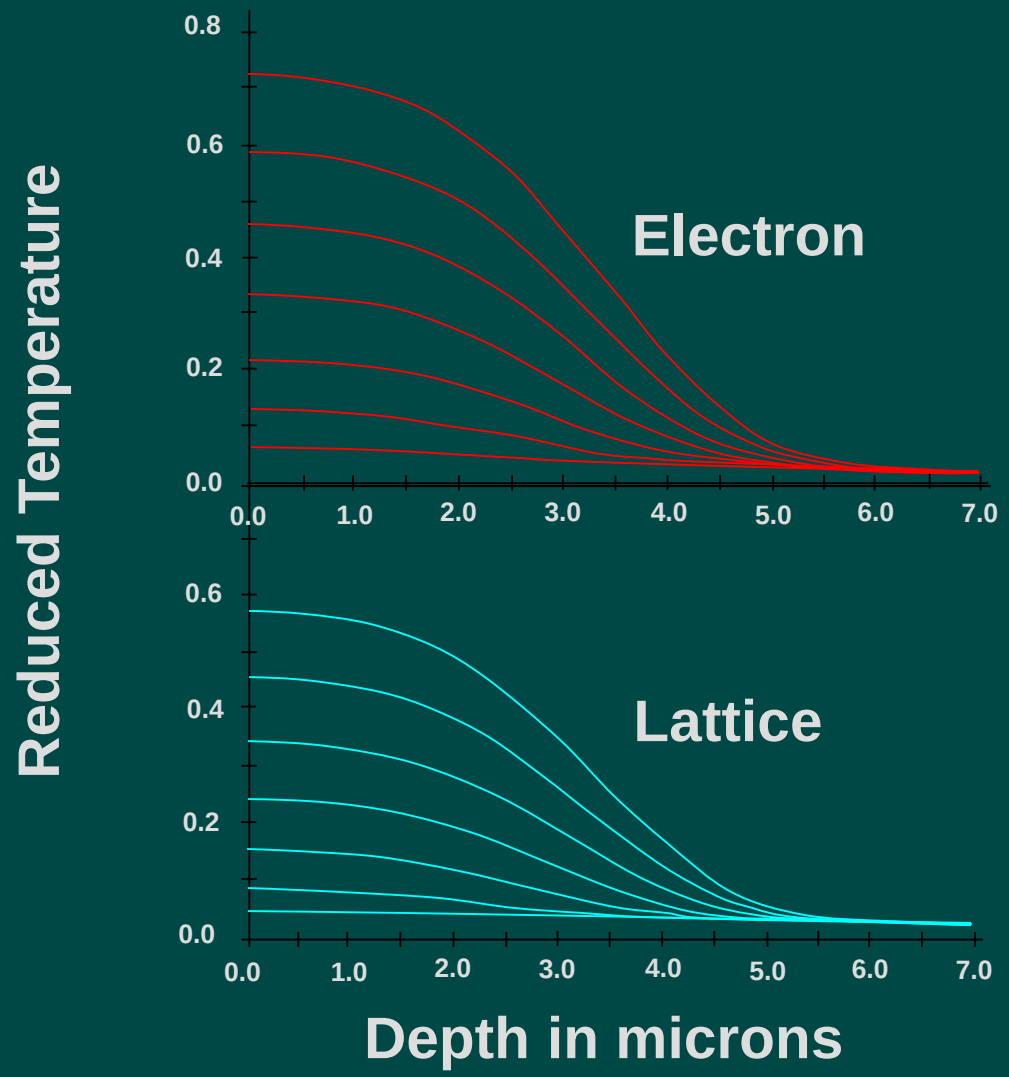

$\Delta t = 0.6\ \mu s$

$\delta = 0.75 \times 10^{8}\ m^{-1}$

$\lambda = 0.4 \times 10^{-7} m$

Surface Temperature Evolution for Aluminium

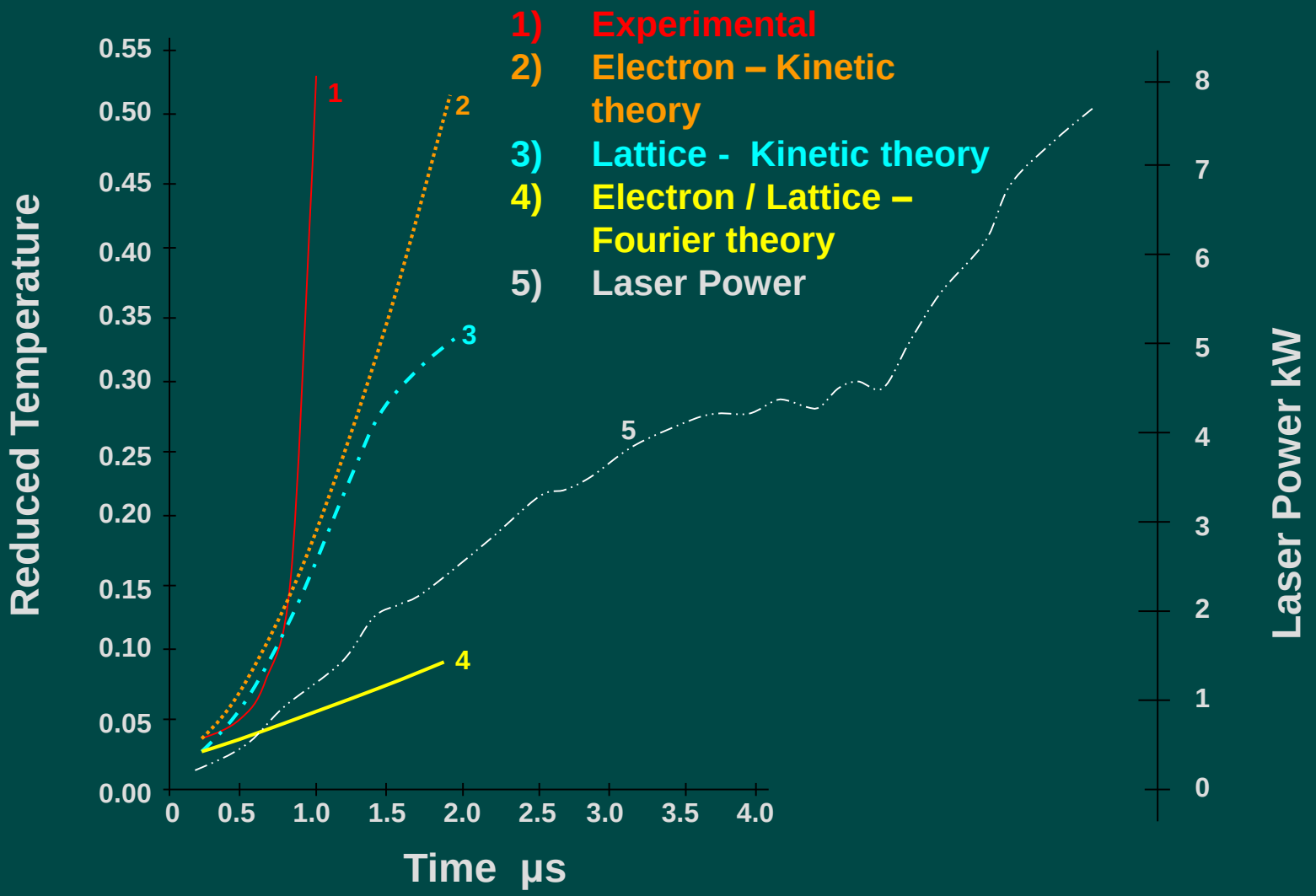

Surface Temperature Evolution for Nickel

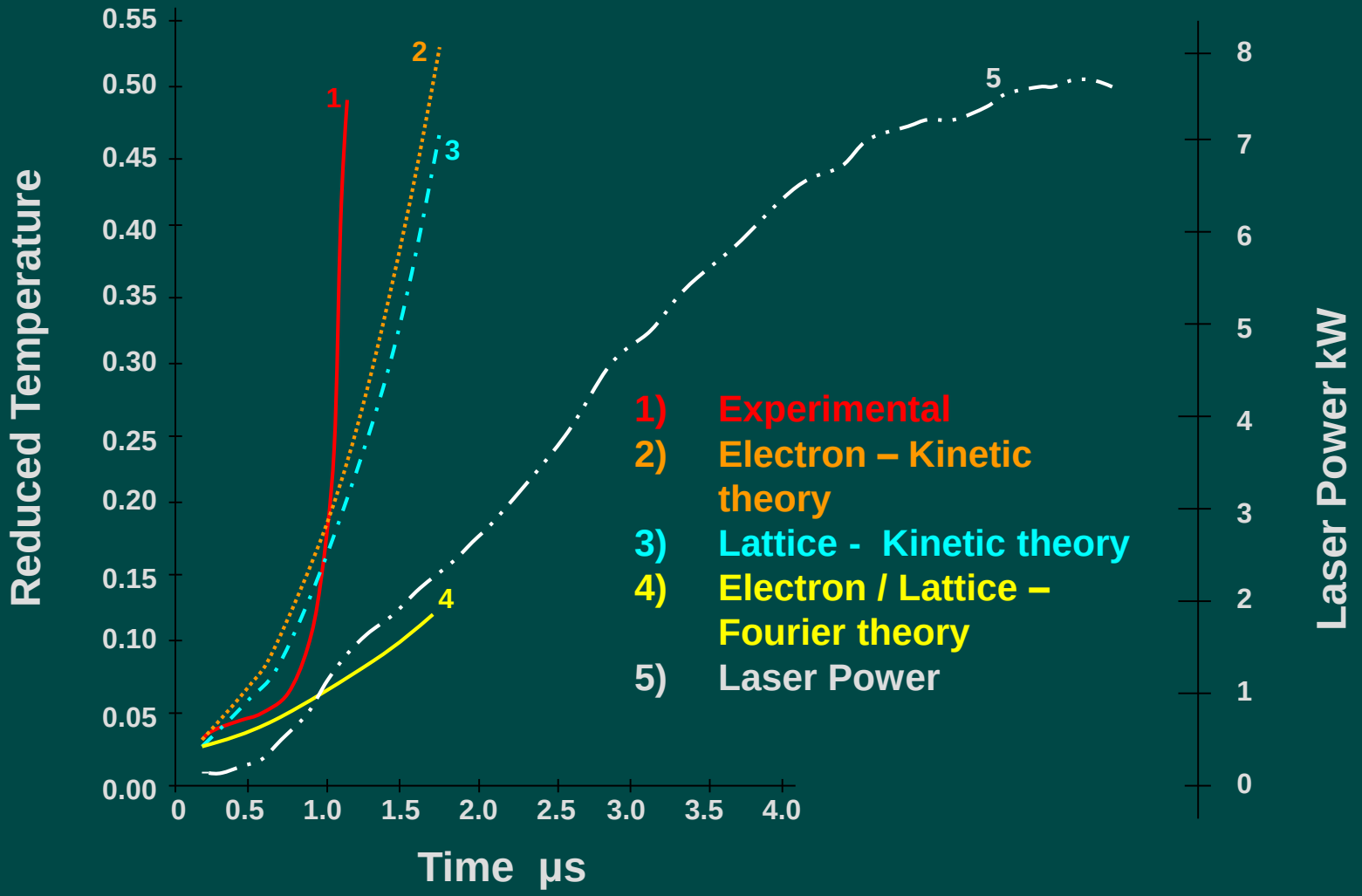

Surface Temperature Evolution for Copper

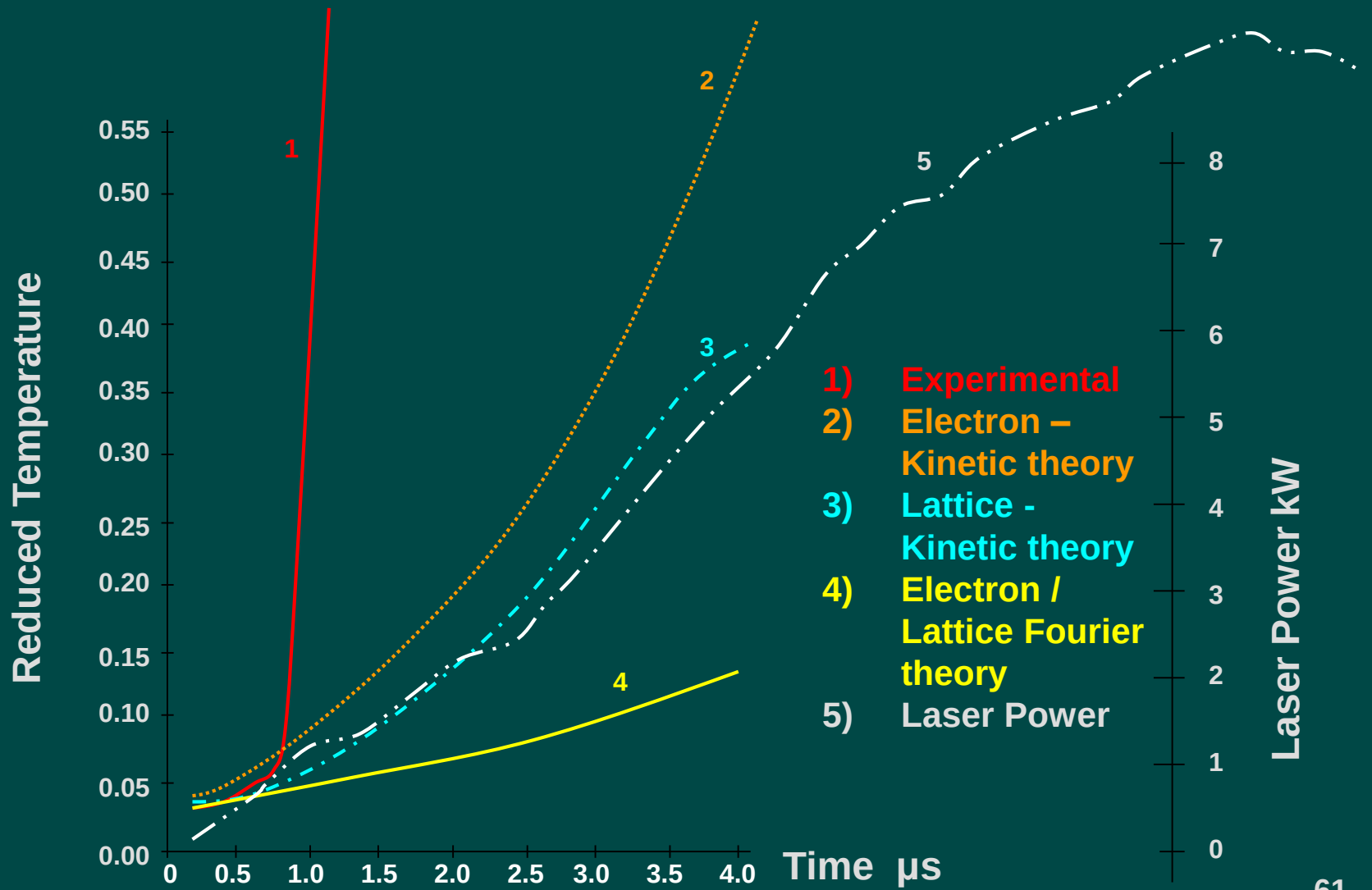

CO_2/CO Laser Facilities in Engineering

AF8P - 8kW Carbon Dioxide Laser can run CW or Pulsed up to 3.3kHz

MFK 1 kW CO_2 Laser

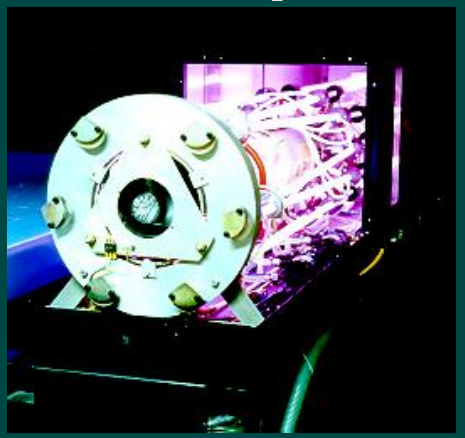

AF8P-CO/01 - 2.5kW Carbon Monoxide Laser can run CW or Pulsed up to 3.3kHz

-Knowledge Based Process Control
-Rapid Prototyping and Tooling
  Laser cutting and Stacking CO_2/CO
-Welding, Cutting, Drilling,
-Laser Bending
-Heat Treatment
-Surface Engineering
  Cladding
  Surface alloying
  Surface texturing
  Laser vapour deposition

Laser Cutting

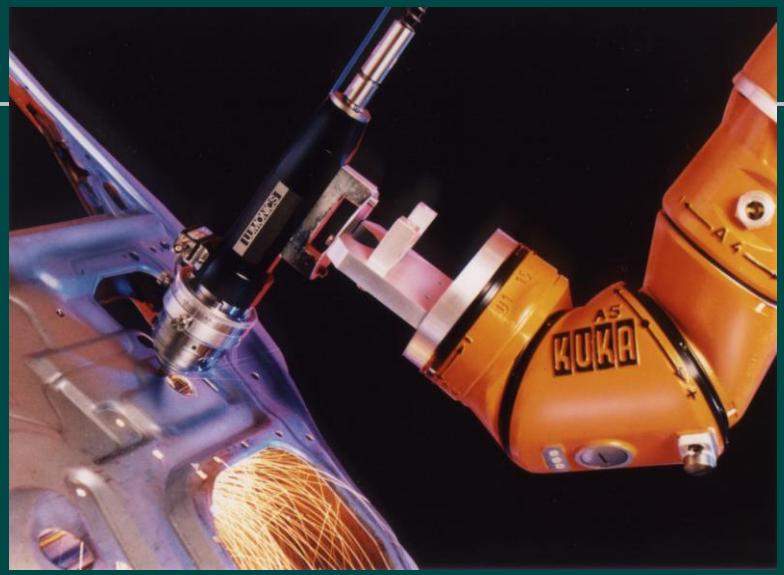

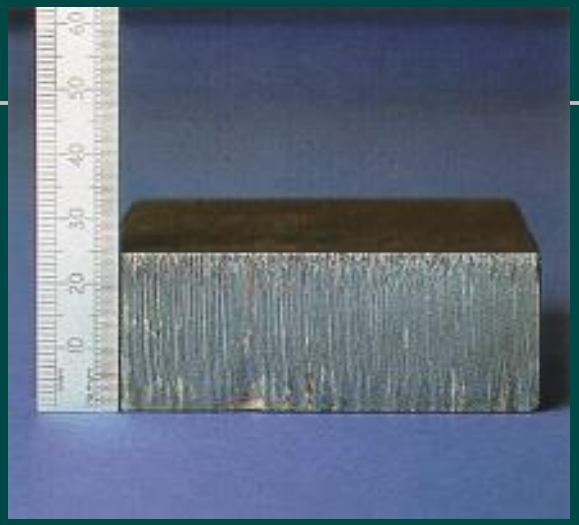

25mm Armour Plate

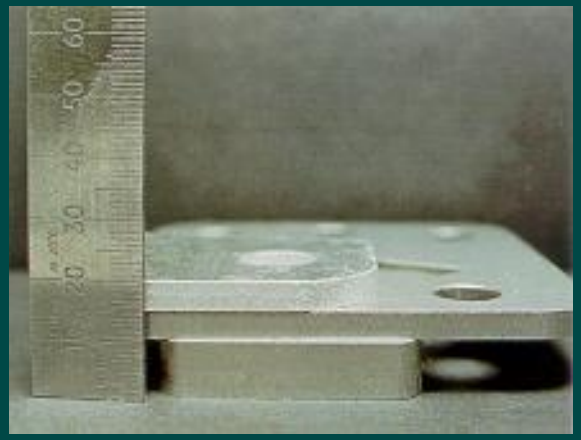

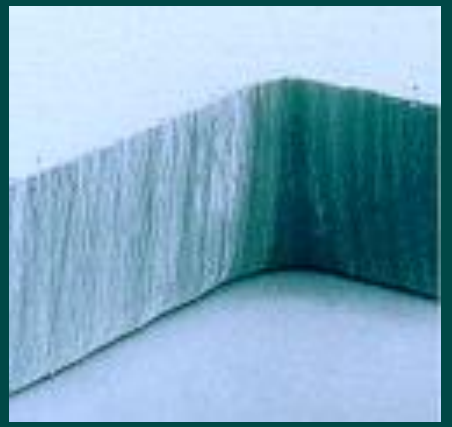

Inert gas (N_2) cut samples of 10 mm stainless, 5 mm stainless, 6 mm aluminium

YAG laser trimming of pressings & CO_2 laser cutting

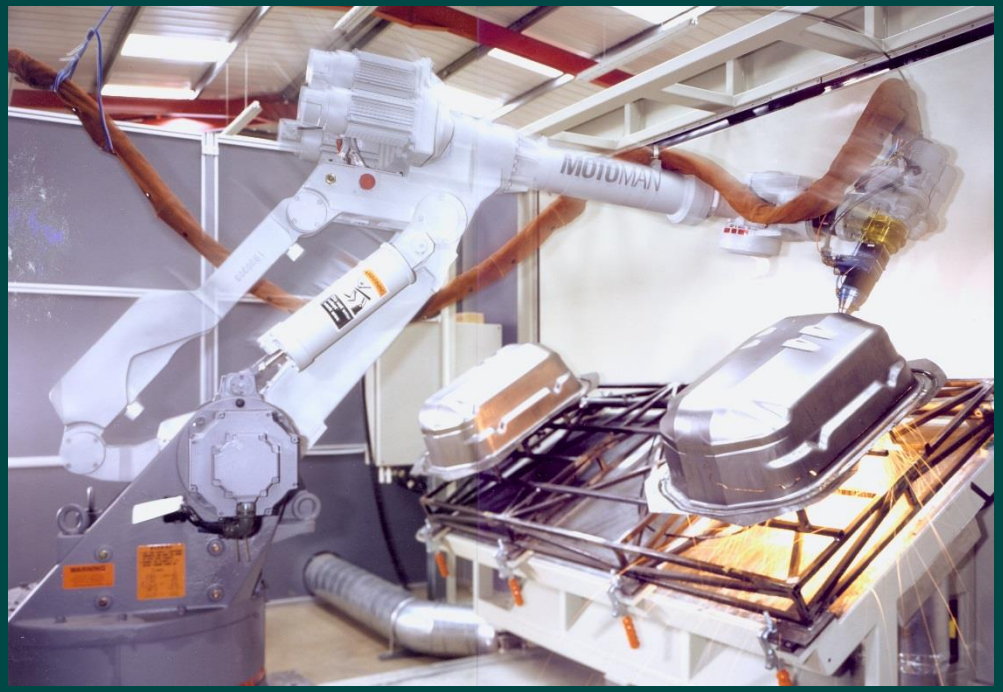

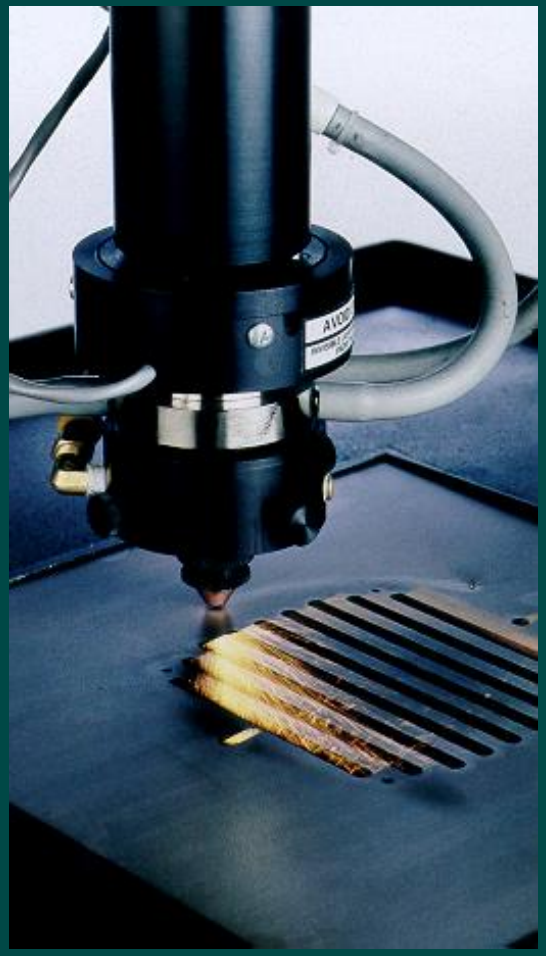

Laser Cutting Nd-YAG & CO_2

Laser cutting of sheet metal is now widely accepted, up to 20 mm thick

Laser cutting of tubes

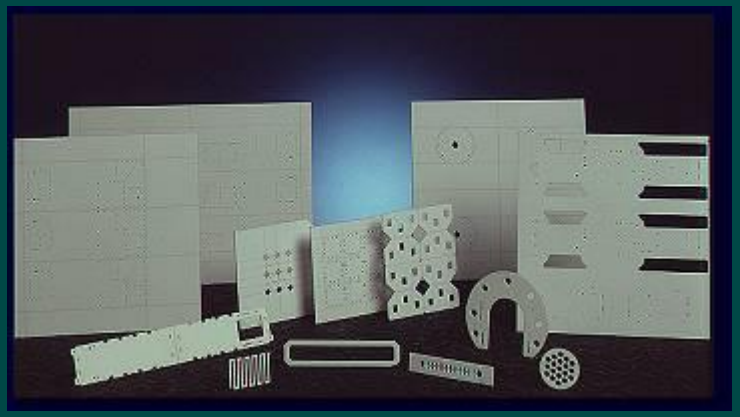

Laser cutting and scribing of ceramics, eg. alumina

Nd-YAG Laser Drilling of Refractory metals

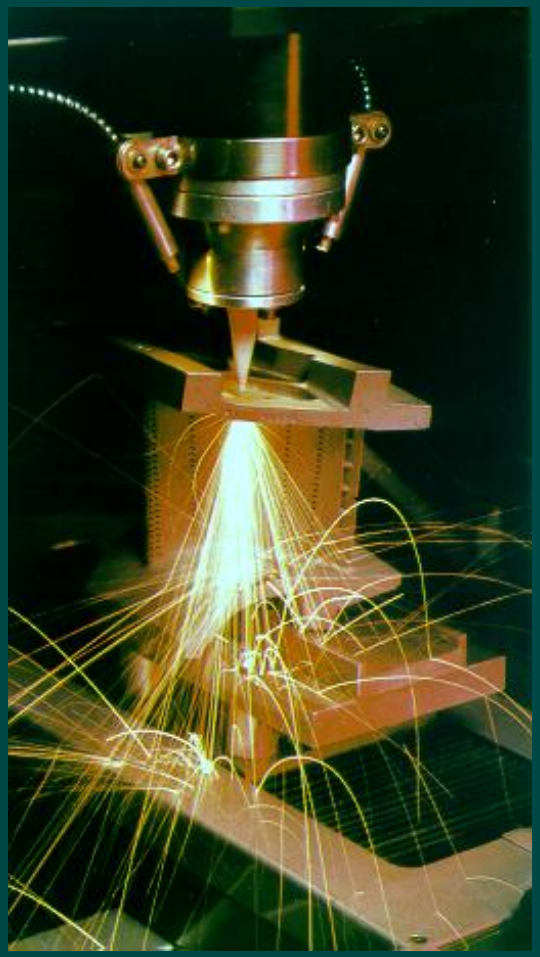

Jet-engine turbine blade
- Nimonic alloy

0.5 mm holes at 20 degrees to the surface
in a jet engine combustion chamber

Excitech Lithographic Micro-machining System 8000

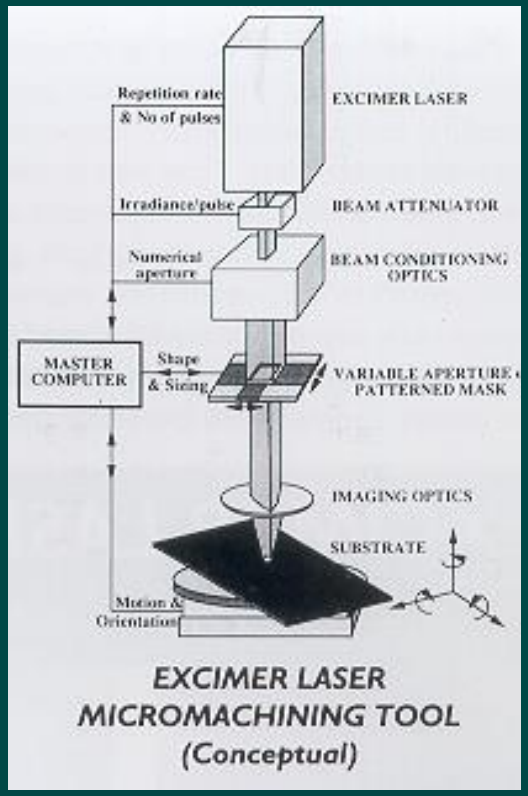

Microstructures in polycarbonate

Mask projection

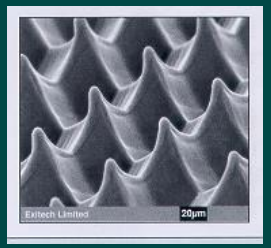

Mask dragging

KrF 248 nm wavelength
ArF 193 nm wavelength

Capable of machining PCB track widths 2 microns wide

CNC controlled and linked into CAD/CAM systems

Structuring of most polymer, ceramic and glass materials

Precise etch depth control to 0.1 microns

Lateral resolution <0.5 microns

Volumetric material removal rate up to $1mm^3/sec$

Example of Fine Processing With Excimer Lasers

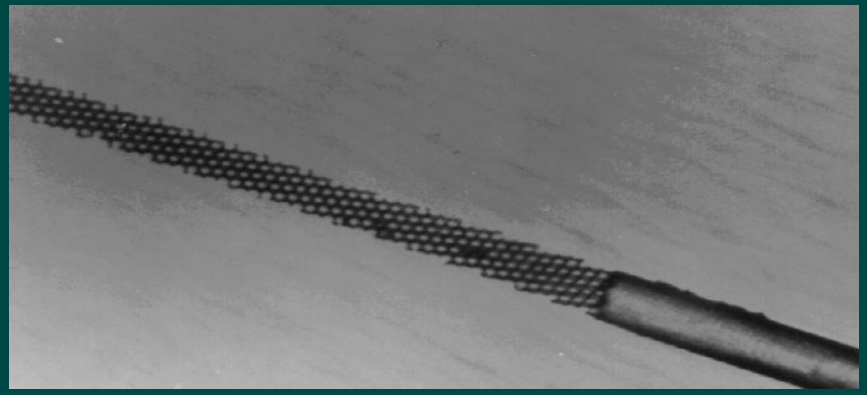

- Hair diameter: ~50 microns (2 thou)
- Hole diameter: ~5 microns (0.2 thou)
- Illustrative of the resolution that can be achieved with a standard excimer laser using the mask-imaging technique and good quality beam delivery optics.

Excimer Laser Micro-Machining - Exitech

PCB Drilling

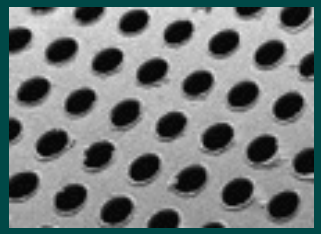

Printer Nozzles

720 dpi nozzle holes

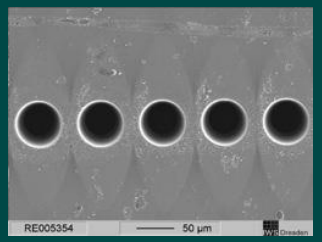

Micro-Fluidic Systems

Biomedical Devices

Microstructuring

Fibre Gratings

Diamond Smoothing

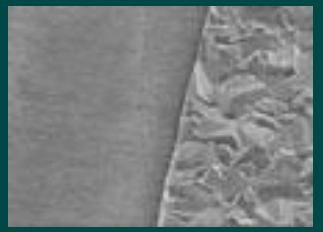

DUV Lithography

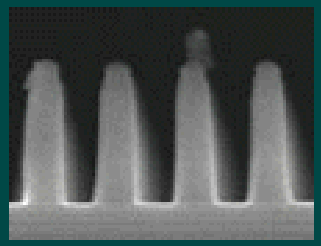

A-R Surface

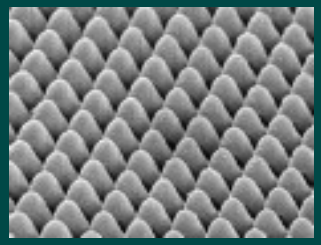

Tapered micro-via

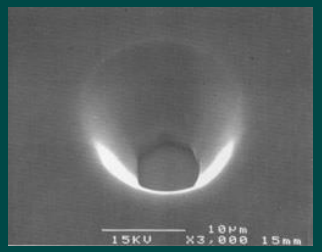

Sensors

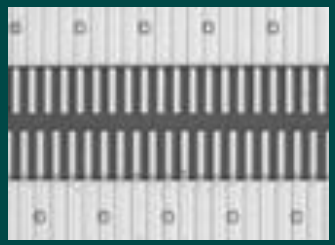

Lab on a Chip

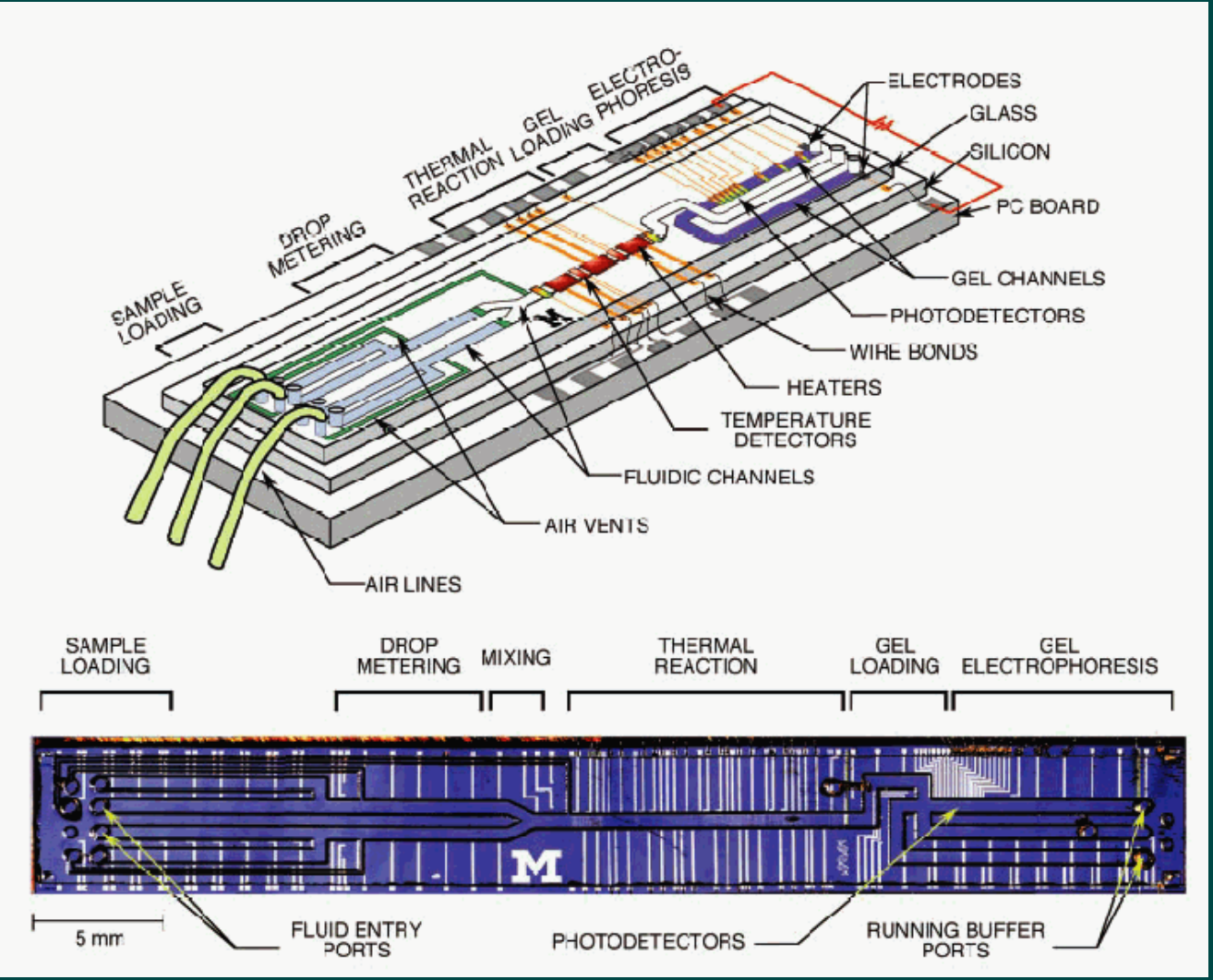
ELECTRODES
GLASS
SILICON
PC BOARD
GEL CHANNELS
PHOTODETECTORS
WIRE BONDS
HEATERS
TEMPERATURE DETECTORS
FLUIDIC CHANNELS
AIR VENTS
AIR LINES
SAMPLE LOADING
DROP METERING
THERMAL REACTION
GEL LOADING
ELECTRO-PHORESIS
SAMPLE LOADING
DROP METERING
MIXING
THERMAL REACTION
GEL LOADING
GEL ELECTROPHORESIS
5 mm
FLUID ENTRY PORTS
PHOTODETECTORS
RUNNING BUFFER PORTS

Blind and Micro-via drilling

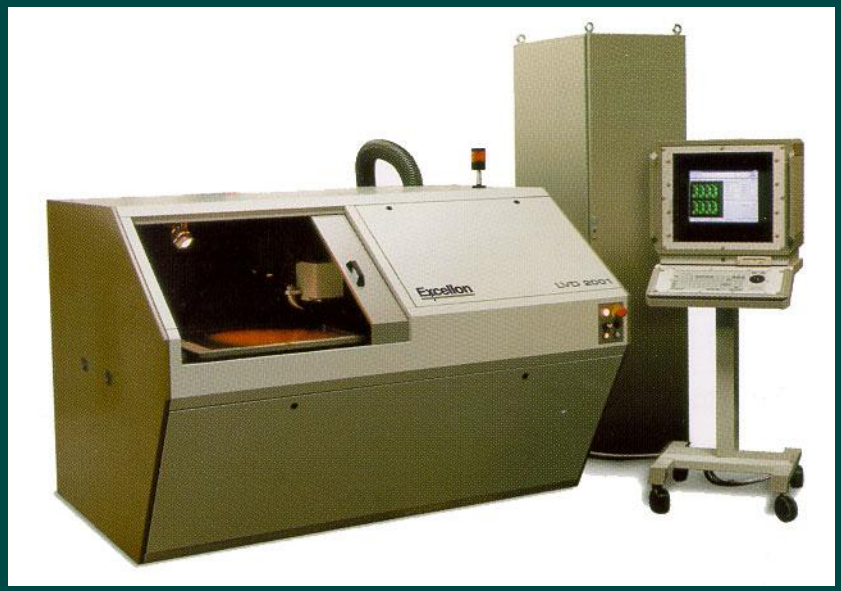

High speed drilling of blind and microvias in all types of multilayer printed circuit boards (PCB's), and multichip modules (MCM's) for panel sizes up to 24" x 28".

Multi Laser (CO_2 /Nd: YAG)

Drills both copper and dielectric

High speed - up to 60,000 holes/minute

The pulsed frequency trippled 3Watt YAG (355nm) laser is used for drilling metals

A wavelength tuned pulsed 80 Watt CO_2 (9.6 microns)laser is used for removal of dielectric

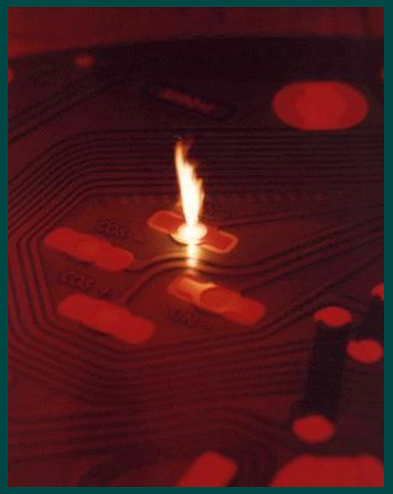

Blind and Micro-via drilling

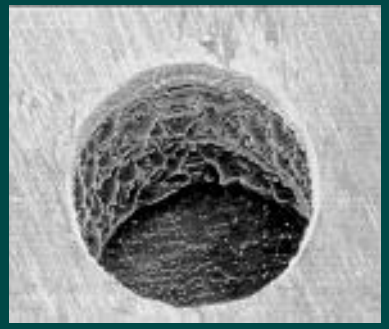

200 μm blind via - 18μm top copper - 125 μm FR4 - laser cleaned bottom copper

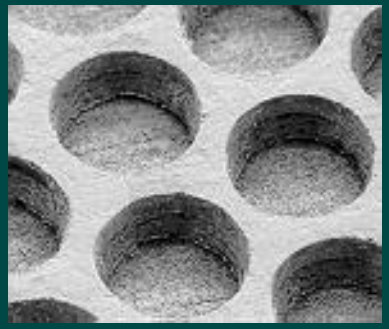

Array of 125 μm blind vias in 25 μm polyimide - pre-patterned top copper

Through holes and annular rings

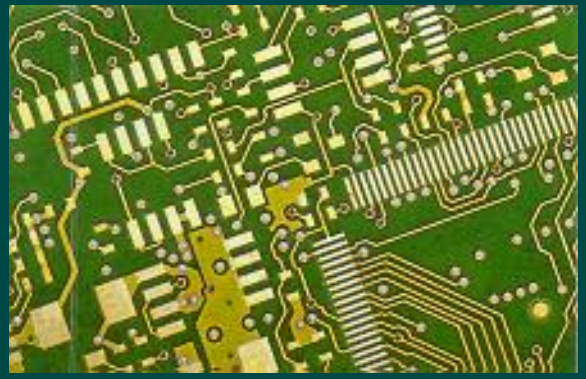

Circuit board blind vias

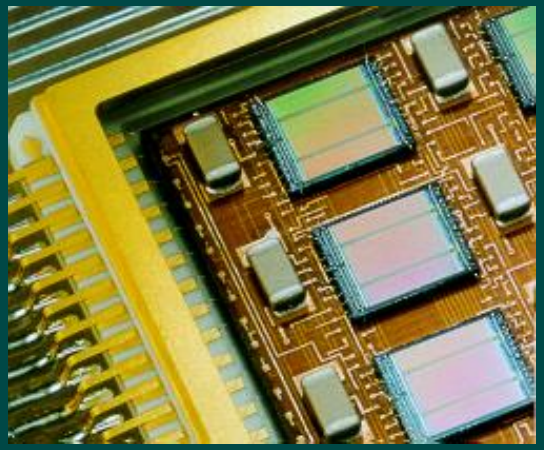

25 μm blind vias

Miniaturised Electronic Products

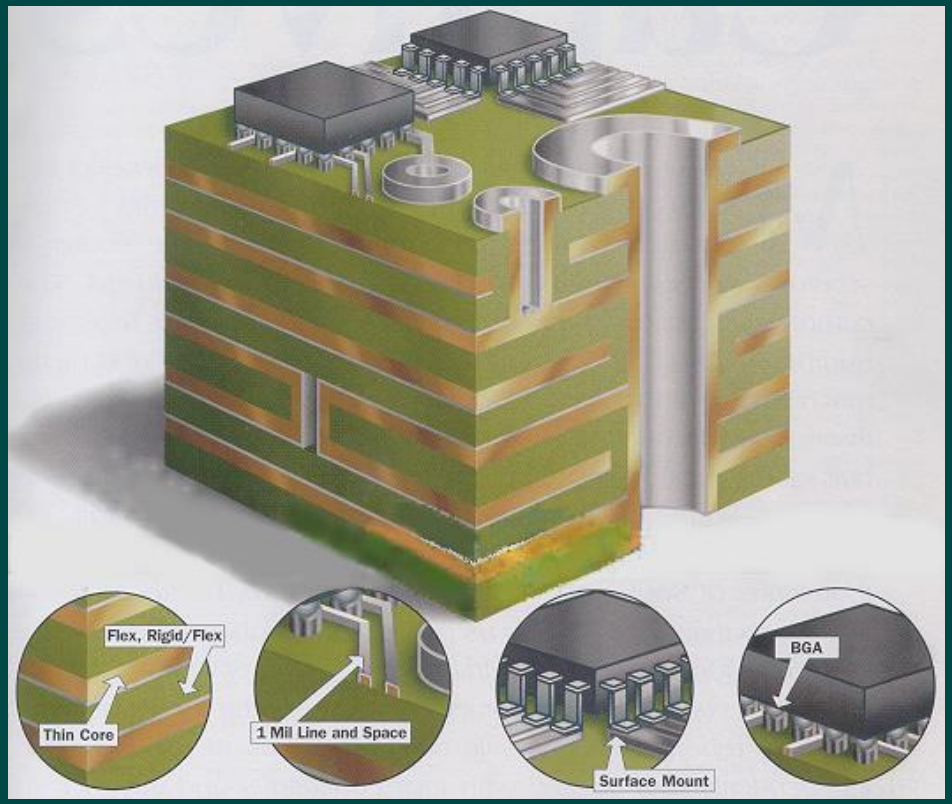

Femtosecond Laser Beam Characteristics

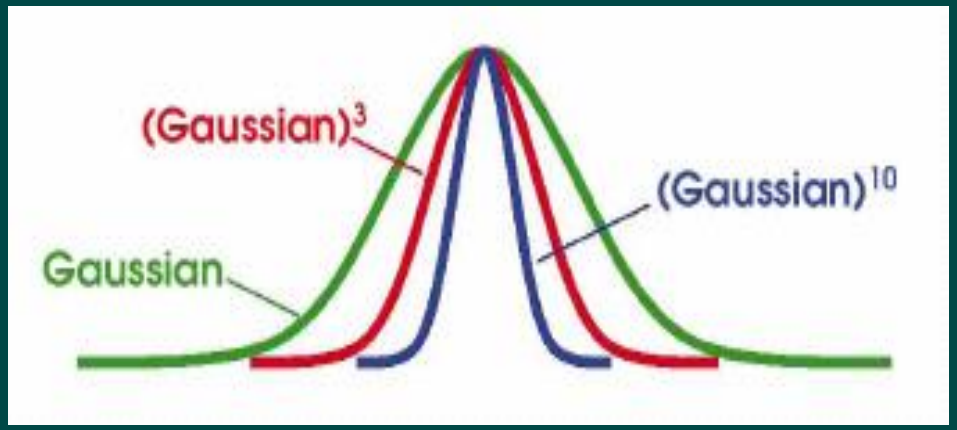

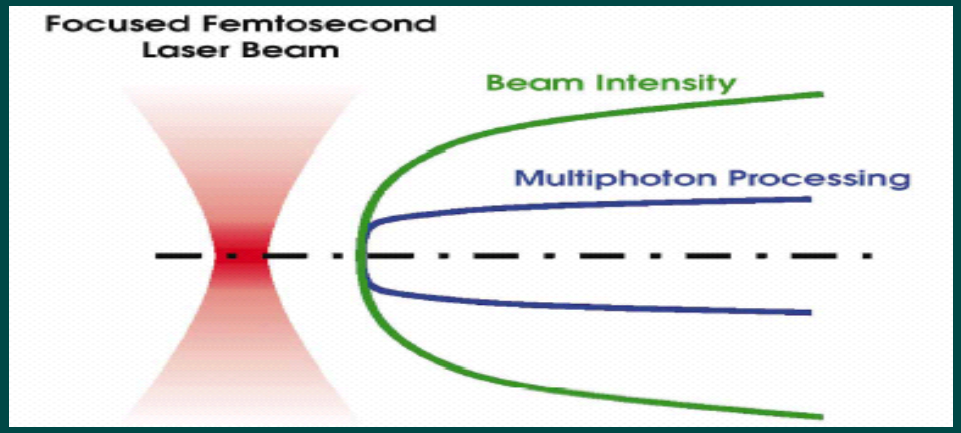

Courtesy of Marco Arrigoni - Coherent

Ti:sapphire lasers with output centred at 800nm have the ability to machine features as small as 70nm. With multi photon absorption, laser power scales as (laser power)^N where N is the number of photons simultaneously absorbed. N ranges from 3 to 10.

Ultra Fast Pulse Interaction

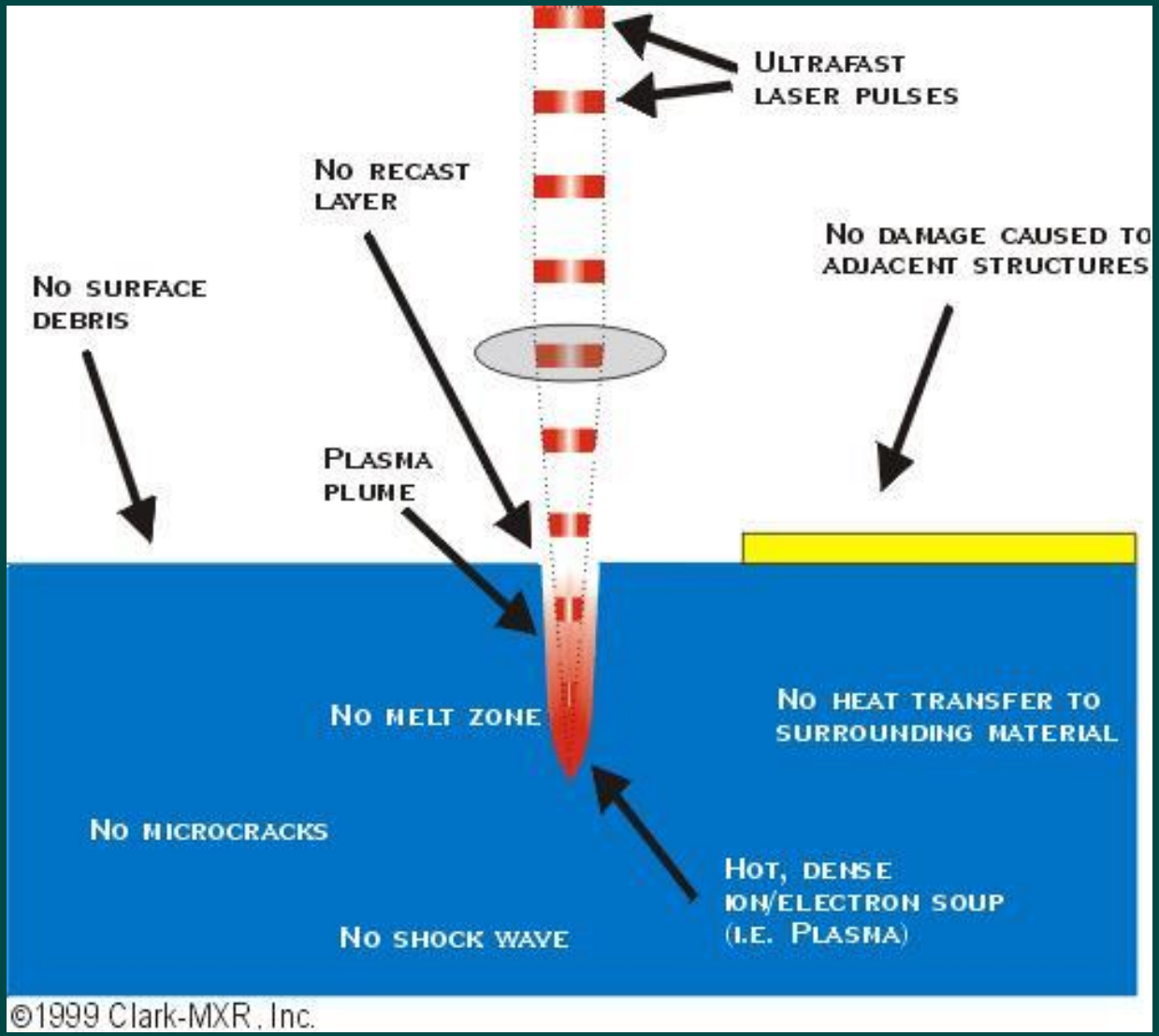

Femtosecond Laser Machining Ti:sapphire - Exitech

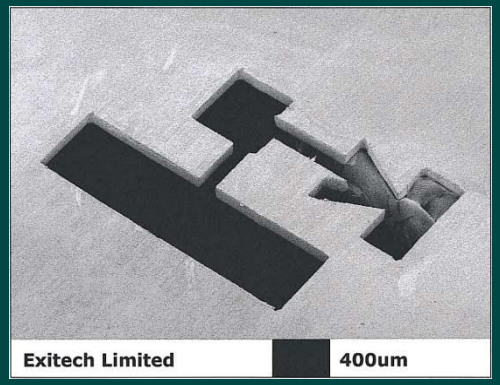

Aluminium

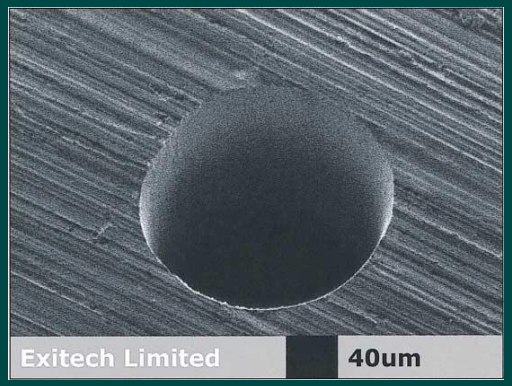

Stainless Steel

100 micron diameter hole drilled in stainless steel using a 355 nm nanosecond pulse Nd: vanadate laser

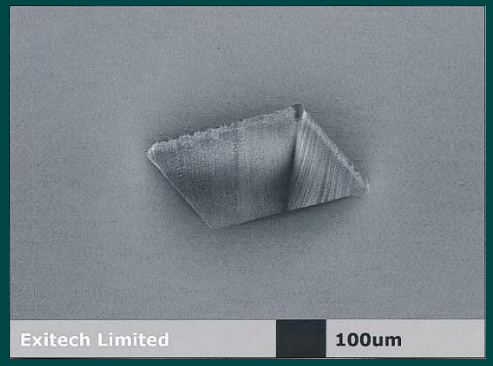

Silica

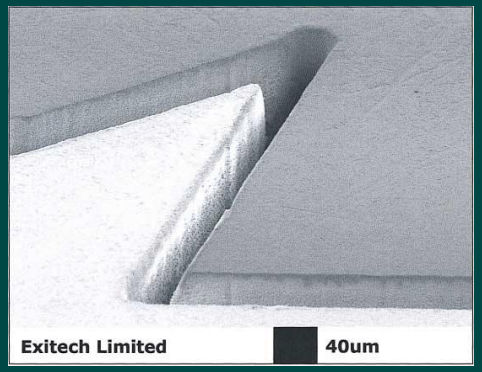

Glass

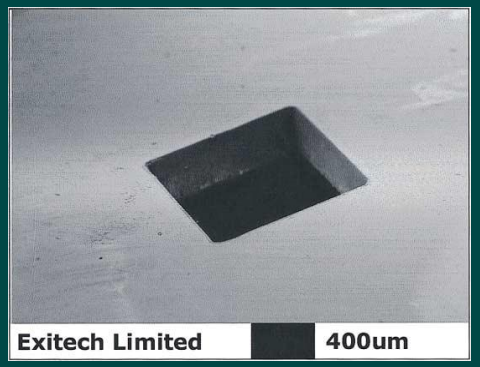

Lithium Tantalate

Ti:sapphire laser; λ_0 ~800 nm, $\Delta\tau$ ~110 fs, E ~1mJ/pulse, Rep Rate ~3–5kHz, $M2$ ~1.2

Precision Percussion Drilling of Stainless Steel - Copper Vapour Laser – Oxford Lasers

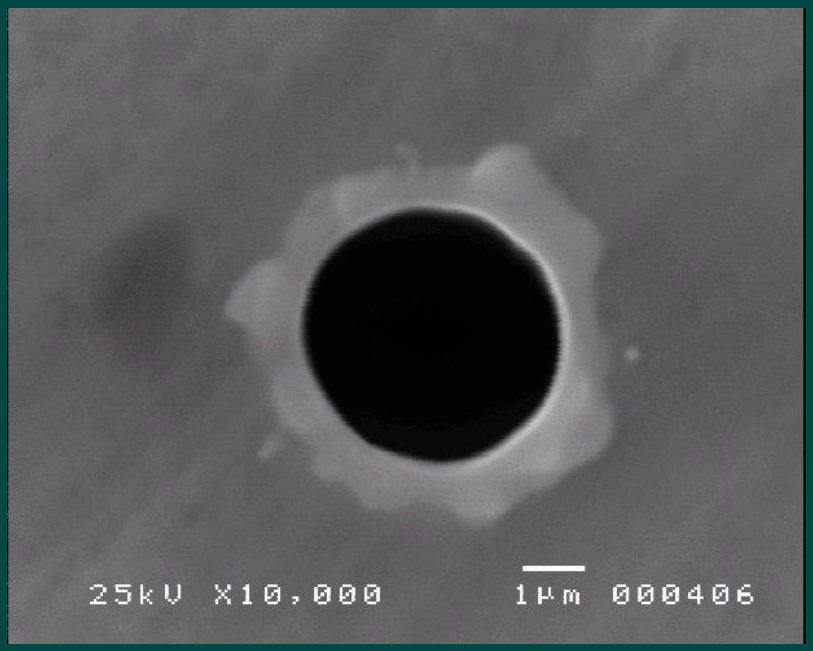

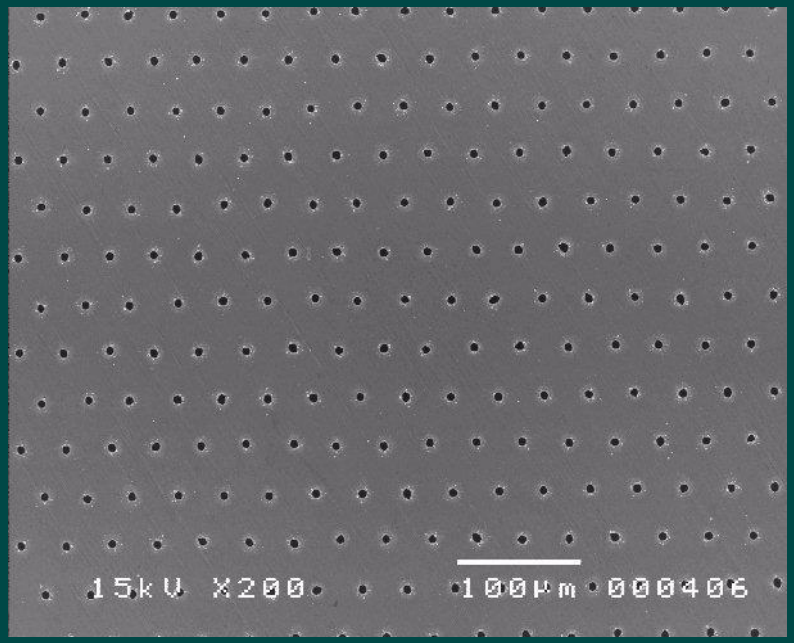

Photograph shows a 22,000 hole array of 5µm diameter holes. Material is stainless steel, 100 µm Copper Vapour Laser , 511 & 578 nm, 10kHz, 20 to 30 ns pulses, 50 to 500 kW

CVL Hole Drilling Capability Table
Oxford Lasers

Diameter – laser exit side (*µm*)	Taper (*µm)*	Thickness (*µm)*	Exit Side Diameter Tolerance (*µm)*
1.5 – 15	+ (5 – 10)	10 – 100	+/- 1
15 – 500	+ (5 – 10)	10 – 200	+/- 0.25 to +/- 1.5
40 – 500	+10 to 0 to -10	200 – 1000	+/- 2 to +/- 4

Precision Holes in CVD Diamond – CVL
(Sample grids for Transmission Electron Microscopes)

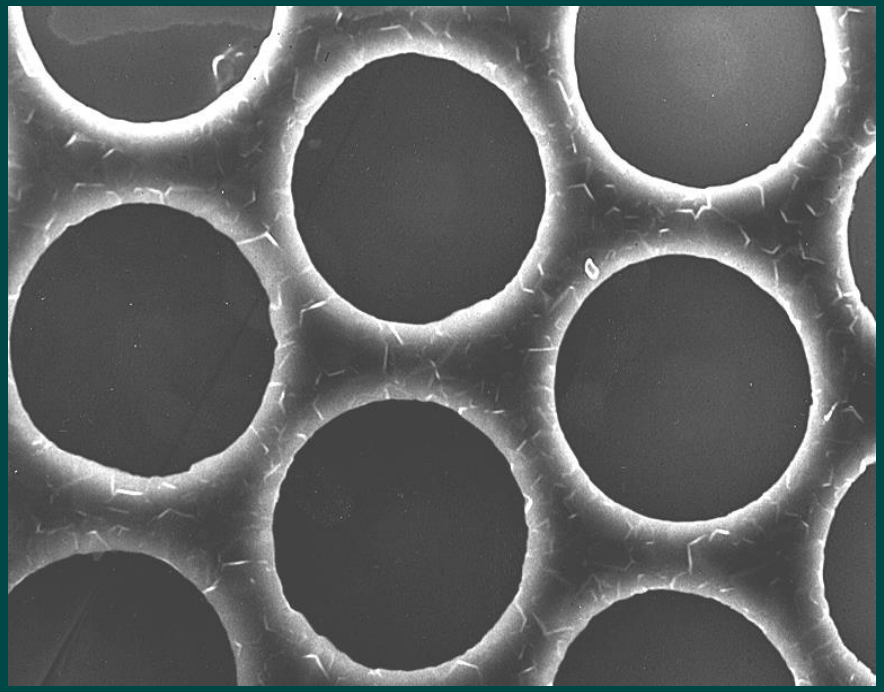

Photograph: An array of precision drilled holes of 230µm diameter on a 295µm pitch in 250 µm thick synthetic diamond.

(Photograph courtesy of GEC-Marconi, Materials Technology Ltd,

References

1. High p.r.f. Nitrogen-Carbon Dioxide Laser for Continuous Manufacturing Processes in Metals: C.R.Chatwin and B.F. Scott. Presented by C.R. Chatwin at the 1st International Conference on Lasers in Manufacturing IFS Publications 1983. Proceedings of 1st International Conference. Edited by Dr.M.F. Kimmitt.
2. Prediction of Output Power from High Pulse Repetition Frequency CO2 Lasers for Use in Manufacturing Processes: C.A.Byabagambi, C.R. Chatwin and B.F. Scott. 3rd International Symposium on Optical and Optoelectronic Applied Sciences and Engineering, High Power Lasers and their Industrial Applications, Innsbruck, Austria. Conference 650, SPIE Proceedings Volume 650, ISBN0-8925262858, 1986.
3. Design of a high p.r.f. carbon dioxide laser for processing high damage threshold materials - C.R. Chatwin, D.W. McDonald, B.F. Scott - SPIE Proceedings, LA, Calif., USA - CO2 Lasers and Applications, January 1989. Vol. 1042, ISBN 0-8194-0077-7, Editors, J.D. Evans, E.V. Locke
4. A 100 kw Mean Power, 10kHz line type pulser for gas laser pumping - D.W. McDonald, C.R. Chatwin, B.F. Scott - SPIE Proceedings, L.A. Calif., USA - Pulse Power for Lasers II - January 1989. Vol. 1046, ISBN 0-8194-0081-5, Editors: T.R. Burkes, G. McDuff.
5. Efficient Laser Power and energy monitoring using an uncoated wedge - C.R. Chatwin, I.A. Watson - Applied Optics, Optical Society of America, Washington, D.C., Jan. 1989, Page 209 to 211.
6. Design of a high p.r.f. carbon dioxide laser for processing high damage threshold materials - C.R. Chatwin, D.W. McDonald, B.F. Scott. Selected Papers on Laser Design, Weichel, H. ed., SPIE Milestone Series 29, (Washington: SPIE Optical Engineering Press, 1991, 425-33) ISBN 08 194 06244
7. Heat flow in materials during melting and resolidification induced by a scanning laser beam - M. Zerroukat, C.R. Chatwin. Numerical Methods in Thermal Problems, Page 32 to 43, Volume VIII, Part 1, Edited by R.W. Lewis, ISBN 0-906674-80-8, Pineridge Press, July 1993
8. Knowledge Control Modelling (KCM) : The Bond Graph Unification Approach to Design and Implementation of an Expert System for Intelligent Industrial Laser Cutting - S.Y. Lim, C.R. Chatwin, H.A. Abdullah. Seventh International Conference on Industrial and Engineering Applications of Artificial Intelligence and Expert Systems, IEA/AIE, Austin, Texas. Editors : F.D. Anger, R.V. Rodriguez, M. Ali, Gordon and Breach Science Publishers, ISBN 2-88449-128-7, Pg. 19-25, May 31 to June 3, 1994
9. Range Control System for Robotically Manipulated Optical Fibre Beam Delivery Systems - H.A. Abdullah, C.R. Chatwin, M.Y. Huang - CLEO Europe 94, 28 August to 2 September, Amsterdam, Netherlands. Sponsored by : EPS, IEEE, OSA, EOS, IOP, IEE; IEEE Catalogue Number : 94TH0614-8; Library of Congress 93-80952; ISBN0-7803-1789-0/SB; ISBN0-7803-1790-4/MF; CThI37, Pg. 326-327, (1994)

References

10. A Pulsed CO2 Laser to Process High Damage Threshold Materials - I.A. Watson, C.R. Chatwin, D.W. McDonald, B.F. Scott - CLEO Europe 94, 28 August - 2 September, Amsterdam, Netherlands. Sponsored by : EPS,IEEE,OSA,EOS,IOP,IEE; IEEE Catalogue No: 94TH0614-8; Library of Congress 93-80952; ISBN0-7803-1789-0/SB; ISBN0-7803-1790-4/MF; CML7, Pg.41-42, (1994).
11. Synthetic Discriminant Filtering Techniques for Laser Cutting Process Control - M Y Huang, C.R. Chatwin, R K Wang - CLEO Europe 94, 28 August - 2 September, Amsterdam, Netherlands. Sponsored by : EPS, IEEE, OSA, EOS, IOP, IEE; IEEE Cataloge No. 94TH0614-8; Library of Congress 93-80952; ISBN 0-7803-1789-0/SB; ISBN0-7803-1790-4/MF; CThA2, Pg.283-284, (1994)
12. Evolutionary Process Prediction and Optimisation for Laser Material Interactions - S.Y. Lim, C.R. Chatwin. Journal of Lasers in Engineering, Gordon & Breach Science, Switzerland, Vol.(2), No.4, 1994, Pg 281 to 299, ISSN 08981507.
13. Computational Moving Boundary Problems - M. Zerroukat, C.R. Chatwin. Research Studies Press - RSP Series : Applied and Engineering Mathematics Series, No. 8, 222 pages, ISBN 0 86380 1684, Marketed by John Wiley & Sons Inc., New York; ISBN 0471951765 May 1994
14. Spatial Chaos Aspects of Laser-Material Interaction - S.Y. Lim, C.R. Chatwin. Journal of Optics and Lasers in Engineering, Elsevier Applied Science, ISSN 0143-8166, Pg. 341-356, Vol.20, No.5 (1994)
15. Intelligent Digital Control of a Laser Cutting Process - S. Y. Lim, C.R. Chatwin. Journal of Lasers in Engineering, Gordon & Breach Science, Switzerland, Vol.3, pp.99-112, ISSN 0898-1507 (1994).
16. Spark Cone Characterisation for Control of Laser Cutting - M.Y. Huang, C.R. Chatwin. Journal of Lasers in Engineering, Gordon & Breach Science, Switzerland, Vol. 3, pp.125-140, ISSN 0898-1507 (1994).
17. Genetic and Entropy Methods for Laser Process Prediction - S. Y. Lim, C.R. Chatwin. Journal of Optics and Lasers in Engineering, Elsevier Applied Science, Vol. 21, No.3, pp. 117-132, ISSN 0143-8166 (1994).
18. Chaos in Laser Material Processing - S.Y. Lim, C.R. Chatwin, Journal of Lasers in Engineering, Gordon & Breach Science, Switzerland, Vol. (3), Pg.43-57, ISSN 0898-1507 (1994).
19. Performance of an Optical Stand-off Control System for Laser & Materials Processing - H.A. Abdullah, C.R. Chatwin, M.Y. Huang - Journal of Optics and Lasers in Engineering, Elsevier Applied Science, Vol.21, No.3, pp.165-180, ISSN 0143-8166 (1994)
20. Non-Linear Heat Flow Computations for CW-Laser-Material Interactions - M. Zerroukat, C.R. Chatwin. Journal of Lasers in Engineering, Gordon & Breach Science, Switzerland, Vol.(3), No.2, Pg.113-123, ISSN0898-1507, Sept.(1994).
21. A Knowledge-Based Adaptive Control Environment for an Industrial Laser Cutting System - M.Y. Huang, C.R. Chatwin - Journal of Optics & Lasers in Engineering, Elsevier Applied Science, Vol.21, No.5, Pg.273-296, ISSN0143-8166, 1994

References

22. Wiener Filter Applied to Laser Cutting Process Control - M.Y. Huang, C.R. Chatwin, R. K. Wang, Lasers in Engineering, Gordon & Breach Science, Switzerland, ISSN0898-1507, Vol.(4), No.1 Pg.1-12 (1995)
23. “Effect of High Power Laser Radiation on Bacteria”. Scottish Microbiology Club, 3rd Symposium, Newcastle upon Tyne, April 1995. Glenn Ward, Ian Watson, Duncan Stewart-Tull, RuiKang Wang, Alastair Wardlaw, Chris Chatwin. RAE Cat: 5, CVCP Cat: 5 Hardness Characteristics of Laser Welded Joints - H.A. Abdullah, C.R. Chatwin, I.A. Watson. CLEO/PACIFIC RIM '95 - Pacific RIM Conference on Lasers and Electro Optics, 11 -14 July, p88, 6 pages, Chiba, Japan; Sponsored by : JSAP, IEICE, IEEE, OSA, OITDA ISBN 0-7803-2400-5 (1995).
24. Segmented ballasted electrodes for a large-volume, sub-atmospheric transverseley excited pulsed laser. I.A. Watson, C.R. Chatwin - Journal of Physics - D: Applied Physics. Pg.258-268, Vol.28, ISSN-0022-3727, (1995).
25. A PID - Knowledge Based System for Non-Linear Process Control - S.Y. Lim, C.R. Chatwin. Invited paper for special issue AI in Automation, Robotics and Computer Vision, Journal of Integrated Computer Aided Engineering, Wiley Interscience, New York, ISSN 1069 2509,Vol. 2, No.4,pp 291 to 298 (1995).
26. De-skilling Industrial Laser Process Development – M.Y. Huang, H.A. Abdullah, C.R. Chatwin – International Journal of Advanced Manufacturing Systems, Springer-Verlag, ISSN 0268-3768, 11: pp 214-220, April (1996).
27. Enhanced Aluminium Processing with a High Frequency, Pulsed $C0_2$ Laser - I.A. Watson, C.R. Chatwin, D McDonald, B.F. Scott, H. A. Abdullah - 14th International Congress on Applications of Lasers and Electro Optics, 80, Laser Institute of America - ICALEO '95, pp 294-302, ISBN 0-912035-53-6, San Diego, California, 13-16 Nov (1995). Published in 1996.
28. Magnetisation Anomalies in Laser Welded Magnetic Materials H.A. Abdullah, I.A. Watson, P. Kapadia, C.R. Chatwin - 14th International Congress on Applications of Lasers & ElectroOptics, Laser Institute of America - ICALEO '95, 964-973, ISBN 0-912035-53-6, San Diego, California, 13-16 November, (1995). Published in 1996.
29. In Process Annealing of Laser Welded High Carbon Steel - H.A. Abdullah. I.A. Watson, C.R. Chatwin - 14th International Congress on Applications of Lasers & Electro-Optics, Laser Institute of America - ICALEO '95, 955-963, ISBN 0- 912035-53-6, San Diego, California, 1316 November, (1995). Published in 1996.
30. Synthetic Discriminant Wiener Filter for In-Process Laser Cutting Quality Control - C.R. Chatwin - Journal of Integrated Computer Aided Engineering, Volume 3, No.(2), pp 129 to 138, March 1996, Wiley Interscience, New York, ISSN 1069 2509.
31. Inactivation of bacteria and yeasts on agar surfaces with high power Nd: YAG laser light - G. D. Ward, I. A. Ward, D. E. S. Stewart-Tull, A. C. Wardlaw, C. R. Chatwin. - Letters in Applied Bacteriology, Vol.23, pp136-140, ISSN 0266 8254, 1996
32. Comparative Bactericidal Activities of Lasers Operating at Seven Different Wavelengths - I. A. Watson, G. D. Ward, R.K.Wang, J. H. Sharp, D. M. Budgett, D. E. Stewart-Tull, A. C. Wardlaw, C. R. Chatwin - Journal of Biomedical Optics, Vol.1 No.(4), pp 466-472, ISSN 1083-3668, Oct. 1996.

References

33. "4 wave Mixing Studies of UV curable resins for micro-stereolithography," Farsari, M., Huang S., Young R.C.D., Chatwin C.R., Heywood M.I; Journal of Photochemistry and Photobiology A: Chemistry 115, ISSN 1010-6030, pg 81-87, 1998
34. Farsari, M., Huang S., Young R.C.D, Heywood M.I., Morrell P.J.B., Chatwin C.R. "Holographic Characterisation of epoxy resins optimised for a wavelength of 351.1nm," SPIE journal of Optical Engineering, Vol 37, No.10, pp.2754-2759, ISSN0091-3286, 1998
35. UV Microstereolithography System Employing Spatial Light Modulator Technology, C.R. Chatwin, M. Farsari, S.-P. Huang, M.I. Heywood, P. Birch, R.C.D. Young, J.D. Richardson, Invited Paper to Special Issue on Spatial Light Modulator Technology, Applied Optics, Vol. 37, No. 32, p. 7514-522, (1998)
36. Characterisation of Epoxy Resins for Microstereolithographic Rapid Prototyping, C.R. Chatwin, M. Farsari, S.-P. Huang, M.I. Heywood, R.C.D. Young, F. Claret-Tournier, J.D. Richardson, International Journal of Advanced Manufacturing Technology, Vol. 15, pp.281-286, 1999
37. Holographic Cure Monitoring of the DuPont Somos™ 7100 Stereolithography Resin, M. Farsari, S.-P. Huang, R.C.D. Young, M.I. Heywood, C.D. Bradfield, C.R. Chatwin, Optics and Lasers in Engineering, Vol. 31, pp. 239-246, 1999
38. Micro-Fabrication using a Spatial Light Modulator in the UV: Experimental Results, M. Farsari, S.-P. Huang, P. Birch, F. Claret-Tournier, R.C.D. Young, C.D. Bradfield, C.R. Chatwin, Optics Letters, Vol. 24, No. 8, pp. 549-550, April 1999
39. H.A. Abdullah, C.R. Chatwin, A.C. Seibi, "Process Optimization Controller for Robotic Laser Machining," Journal of Laser Applications, Laser Institute of America, ISSN 1042-346X, pp263-267, No.6, Vol.11, December 1999
40. Micro-Fabrication Employing High-Resolution Imaging Stereolithography, C.R. Chatwin, M. Farsari, F. Claret-Tournier, S.-P. Huang, P.M. Birch, R.C.D. Young, D.M. Budgett, J.D. Richardson, Lasers in Manufacturing, Vol. 15, pp. 31-33, 1999
41. A Novel High-Accuracy Microstereolithography Method Employing An Adaptive Electro-Optic Mask, M. Farsari, F. Claret-Tournier, S-P. Huang, C. R. Chatwin, D.M. Budgett, P. M. Birch, R. C. D. Young, J. D. Richardson, Journal of Materials Processing Technology, Vol. 107(1-3), pp. 167-172, 2000.
42. C.R. Chatwin, " Carbon Dioxide Laser", Encyclopedia of Modern Optics, Elsevier Academic Press - Physics, Editor R. D. Guenther, Page 389-400, ISBN 0-12-227600-0, 2004.

The End